12 December 2017

Dr. Nathalie Combourieu-Nebout, Editor Climate of the Past

Resubmission of Manuscript (Ref. No. cp-2017-104)

Dear Nathalie,

Thank so much for accepting our manuscript entitled "*Holocene climate aridification trend and human impact interrupted by millennial- and centennial-scale climate fluctuations from a new sedimentary record from Padul (Sierra Nevada, southern Iberian Peninsula)*", authored by María J. Ramos-Román, Gonzalo Jiménez-Moreno, Jon Camuera, Antonio García-Alix, R. Scott Anderson, Francisco J. Jiménez-Espejo, José S. Carrión, for publication in Climate of the Past. Here we are resubmitting the manuscript with some final corrections suggested by you of our previously submitted version of the manuscript (cp-2017-104).

We hope you find merit in this work and we look forward to hearing from you.

María J. Ramos-Román

Departamento de Estratigrafía y Paleontología

Universidad de Granada, Spain

Author's responses to the editor:

The editor suggestions and comments are displayed in black, and our answers are in blue. We indicate the lines in which we made the modifications according to the marked-up manuscript version (see below).

Editor Decision: Publish subject to minor revisions (review by editor) (04 Dec 2017) by Nathalie Combourieu Nebout

Comments to the Author:
Dear authors,

I had a look on your response and you corrections and I would like some additional amendments before a definitive acceptance of your manuscript.

The first point is what you say for figure 6. I do not agree with you. The scale is very important here as you base your demonstration on very low percentages lower that 10 % concerning the Botryococcus. Curves are too much magnified comparing to other curves (4 % of them represent 10 % of Mediterranean taxa.) and the curve of IRD has also to be restrained to reasonable proportions. The reader will probably see the same but he(she) see that in a reasonable presentation of the variations of the different proxies comparing to other data presented on the right of the figure. So I suggest you to moderate the scale of the pollen and IRD curves in figure 6. Please do that before acceptance. Thank you.

Ok, we modified considerably the scale of pollen and IRD as you suggested. We hope you are now satisfied with this figure.

The second point concerns the charcoal data. I have understand what you say about the analyses in progress which are part of a master. In fact I do not ask you to publish any original data on charcoal analyses. What I propose to you to respond to two of the reviewers is only to place one or two sentences indicating tthat first preliminary data seem to confirm or not one or another point concerning the low impact of Human on the vegetation in the whole part of the diagram (up to 1500 yr) without detailing the data (writing name of the student and his professor, personal communication). As the man who drives this master is one co-author of your paper, such short amendment will be the best thing to do and it is really important for your

paper to mention that in your discussion in order to reinforce the climate driving of your results as you point that in the abstract as one of the main results. You may also add the name of the student if necessary in the author list. Please add something like that in the discussion with the mention "personal communication". Thank you

Ok, we added some information about the preliminary charcoal analysis, which agree with the pollen analysis in showing little human impact in the area until very recent. Please see modification in lines 711-717.

These minor changes will not take too many time to do. I am waiting after the new version of you manuscript.

with my best regards

Nathalie Combourieu-Nebout

Thank you very much.
Best regards,

María J. Ramos-Román

1 **Holocene climate aridification trend and human impact interrupted by millennial- and**
2 **centennial-scale climate fluctuations from a new sedimentary record from Padul (Sierra**
3 **Nevada, southern Iberian Peninsula)**

4 María J. Ramos-Román[1], Gonzalo Jiménez-Moreno[1], Jon Camuera[1], Antonio García-Alix[1],
5 R. Scott Anderson[2], Francisco J. Jiménez-Espejo[3], José S. Carrión[4]

6 [1] Departamento de Estratigrafía y Paleontología, Universidad de Granada, Spain
7 [2] School of Earth Sciences and Environmental Sustainability, Northern Arizona University,
8 USA.
9 [3] Department of Biogeochemistry, Japan Agency for Marine-Earth Science and Technology
10 (JAMSTEC), Japan.
11 [4] Departamento de Biología Vegetal, Facultad de Biología, Universidad de Murcia, Murcia,
12 Spain.

13 *Correspondence to:* María J. Ramos-Román (mjrr@ugr.es)

14 **Abstract.** Holocene centennial-scale paleoenvironmental variability has been described in a
15 multiproxy analysis (i.e. lithology, geochemistry, macrofossil and microfossil analyses) of a
16 paleoecological record from the Padul basin in Sierra Nevada, southern Iberian Peninsula.
17 This sequence covers a relevant time interval hitherto unreported in the studies of the Padul
18 sedimentary sequence. The ~4700 yr-long record has preserved proxies of climate variability,
19 with vegetation, lake levels and sedimentological change during the Holocene in one of the
20 most unique and southernmost wetland from Europe. The progressive Middle and Late
21 Holocene trend toward arid conditions identified by numerous authors in the western
22 Mediterranean region, mostly related to a decrease in summer insolation, is also documented
23 in this record, being here also superimposed by centennial-scale variability in humidity. In
24 turn, this record shows centennial-scale climate oscillations in temperature that correlate with
25 well-known climatic events during the Late Holocene in the western Mediterranean region,
26 synchronous with variability in solar and atmospheric dynamics. The multiproxy Padul
27 record first shows a transition from a relatively humid Middle Holocene in the western
28 Mediterranean region to more aridity from ~4700 to ~2800 cal yr BP. A relatively warm and
29 humid period occurred between ~2600 to ~1600 cal yr BP, coinciding with persistent
30 negative NAO conditions and the historic Iberian-Roman Humid Period. Enhanced arid
31 conditions, co-occurring with overall positive NAO conditions and increasing solar activity,
32 are observed between ~1550 to ~ 450 cal yr BP (~400 to ~1400 CE) and colder and warmer
33 conditions happened during the Dark Ages and Medieval Climate Anomaly, respectively.
34 Slightly wetter conditions took place during the end of the MCA and the first part of the
35 Little Ice Age, which could be related to a change towards negative NAO conditions and
36 minima in solar activity. Time series analysis performed from local (*Botryococcus* and TOC)
37 and regional (Mediterranean forest) signals helped us determining the relationship between
38 southern Iberian climate evolution, atmospheric, oceanic dynamics and solar activity. Our
39 multiproxy record shows little evidence of human impact in the area until ~1550 cal yr BP,
40 when evidence of agriculture and livestock grazing occurs. Therefore climate is the main
41 forcing mechanism controlling environmental change in the area until relatively recently.

43 **Keywords:** Holocene, Padul**,** peat bog, North Atlantic Oscillation, atmospheric dynamics,
44 southern Iberian Peninsula, Sierra Nevada, western Mediterranean.

1 Introduction

The Mediterranean area is situated in a sensitive region between temperate and subtropical climates making it an important place to study the connections between atmospheric and oceanic dynamics and environmental change. Climate in the western Mediterranean and the southern Iberian Peninsula is influenced by several atmospheric and oceanic dynamics (Alpert et al., 2006), including the North Atlantic Oscillation (NAO) one of the principal atmospheric phenomenon controlling climate in the area (Hurrell, 1995; Moreno et al., 2005). Recent NAO reconstructions in the western Mediterranean relate negative and positive NAO conditions with an increase and decrease, respectively, in winter (effective) precipitation (Olsen et al., 2012; Trouet et al., 2009). Numerous paleoenvironmental studies in the western Mediterranean have detected a link at millennial- and centennial-scales between the oscillations of paleoclimate proxies from sedimentary records with solar variability and atmospheric (i.e., NAO) and/or ocean dynamics during the Holocene (Fletcher et al., 2013; Moreno et al., 2012; Rodrigo-Gámiz et al., 2014). Very few montane and low altitude lake records in southern Iberia document centennial-scale climate change [see, for example Zoñar Lake (Martín-Puertas et al., 2008)], with most terrestrial records in the western Mediterranean region evidencing only millennial-scale cyclical changes. Therefore, higher-resolution decadal-scale analyses are necessary to analyze the link between solar activity, atmospheric and oceanographic systems with terrestrial environment in this area at shorter (i.e., centennial) time scales.

Sediments from lakes, peat bogs and marine records from the western Mediterranean have documented an aridification trend during the Late Holocene (Carrión et al., 2010; Gil-Romera et al., 2010; Jalut et al., 2009). This trend, however, was superimposed by shorter-term climate variability, as shown by several recent studies from the region (Carrión, 2002; Fletcher et al., 2013; Jiménez-Moreno et al., 2013; Martín-Puertas et al., 2008; Ramos-Román et al., 2016). This relationship between climate variability, culture evolution and human impact during the Late Holocene has also been the subject of recent paleoenvironmental studies (Carrión et al., 2007; Lillios et al., 2016; López-Sáez et al., 2014; Magny, 2004). However, it is still unclear whether climate or human activities have been the main forcing driving environmental change (i.e., deforestation) in this area during this time.

Within the western Mediterranean, Sierra Nevada is the highest and southernmost mountain range in the Iberian Peninsula and thus presents a critical area for paleoenvironmental studies. Most high-resolution studies there have come from high elevation sites. The well-known Padul wetland site is located at the western foot of the Sierra Nevada (Fig. 1) and bears one of the longest continental records in southern Europe, with a sedimentary sequence of ~100 m thick that could represent the last 1 Ma (Ortiz et al., 2004). Several research studies, including radiocarbon dating, geochemistry and pollen analyses, have been carried out on previous cores from Padul, and have documented glacial/interglacial cycles during the Pleistocene and up until the Middle Holocene. However, the Late Holocene section of the Padul sedimentary sequence has never been effectively retrieved and studied (Florschütz et al., 1971; Ortiz et al., 2004; Pons and Reille, 1988). This was due to the location of these previous corings within a current peat mine operation, where the upper (and non- productive) part of the sedimentary sequence was missing.

Here we present a new record from the Padul basin: Padul-15-05, a 42.64 m-long sediment core that, for the first time, contains a continuous record of the Late Holocene (Fig. 2). A high-resolution multi-proxy analysis of the upper 1.15 m, the past ~4700 cal yr BP, has

94 allowed us to determine a complete paleoenvironmental and paleoclimatic record at
95 centennial- and millennial-scales. To accomplish that, we reconstructed changes in the Padul
96 vegetation, sedimentation, climate and human impact during the Holocene throughout the
97 interpretation of the lithology, palynology and geochemistry.

99 Specifically, the main objective of this paper is to determine environmental variability and
100 climate evolution in the southern Iberian Peninsula and the western Mediterranean region and
101 their linkages to northern hemisphere climate and solar variability during the latter Holocene.
102 In order to do this, we compared our results with other paleoclimate records from the region
103 and solar activity from the northern hemisphere for the past ~4700 cal yr BP (Bond et al.,
104 2001; Laskar et al., 2004; Sicre et al., 2016; Steinhilber et al., 2009).

2 Regional setting: Padul, climate and vegetation

106 Padul is located at the foothill of Sierra Nevada, which is a W-E aligned mountain range
107 located in Andalucía (southern Spain; Fig. 1). Climate in this area is Mediterranean, with cool
108 and humid winters and hot/warm summer drought. Sierra Nevada is strongly influenced by
109 thermal and precipitation variations due to the altitudinal gradient (from ca. 700 to more than
110 3400 m), which control plant taxa distribution in different bioclimatic vegetation belts due to
111 the variability in thermotypes and ombrotypes (Valle Tendero, 2004). According to the
112 climatophilous series classification, Sierra Nevada is divided in four different vegetation belts
113 (Fig. 1). The crioromediterranean vegetation belt, occurring above ~2800 m, is characterized
114 by tundra vegetation and principally composed by species of Poaceae, Asteraceae,
115 Brassicaceae, Gentianaceae, Scrophulariaceae and Plantaginaceae between other herbs, with
116 a number of endemic plants (e.g. *Erigeron frigidus, Saxifraga nevadensis, Viola crassiuscula,*
117 *Plantago nivalis*). The oromediterranean belt, between ~ 1900 to ~2800 m, is principally
118 made up of *Pinus sylvestris*, *P. nigra* and *Juniperus* spp. and other shrubs such as species of
119 Fabaceae, Cistaceae and Brassicaceae. The supramediterranean belt, from ~ 1400 to 1900 m
120 of elevation, bears principally *Quercus pyrenaica*, *Q. faginea* and *Q. rotundifolia* and *Acer*
121 *opalus* ssp. *granatense* with other trees and shrubs, including members of the Fabaceae,
122 Thymelaeaceae, Cistaceae and *Artemisia* sp. being the most important. The
123 mesomediterranean vegetation belt occurs between ~600 and 1400 m of elevation and is
124 principally characterized by *Quercus rotundifolia*, some shrubs, herbs and plants as *Juniperus*
125 sp., and some species of Fabaceae, Cistaceae and Liliaceae with others (El Aallali et al.,
126 1998; Valle, 2003). The human impact over this area, especially important during the last
127 millennium, affected the natural vegetation distribution through fire, deforestation,
128 cultivation (i.e., *Olea*) and subsequent reforestation (mostly *Pinus*) (Anderson et al., 2011).
129 The Padul basin is situated in the mesomediterranean vegetation belt at approximately 725 m
130 elevation in the southeastern part of the Granada Basin. In this area and besides the
131 characteristic vegetation at this elevation, nitrophilous communities occur in soils disrupted
132 by livestock, pathways or open forest, normally related with anthropization (Valle, 2003).
133 This is one of the most seismically active areas in the southern Iberian Peninsula with
134 numerous faults in NW-SE direction, with the Padul fault being one of these active normal
135 faults (Alfaro et al., 2001). It is a small extensional basin approximately 12 km long and
136 covering an area of approximately 45 km^2, which is bounded by the Padul normal fault. The
137 sedimentary in-filling of the basin consists of Neogene and Quaternary deposits; Upper
138 Miocene conglomerates, calcarenites and marls, and Pliocene and Quaternary alluvial
139 sediments, lacustrine and peat bog deposits (Sanz de Galdeano et al., 1998; Delgado et al.,
140 2002; Domingo et al., 1983).

141
142 The Padul wetland is endorheic, with a surface of approximately 4 km^2 placed in the Padul
143 basin that contains a sedimentary sequence characterized mostly by peat accumulation. The
144 basin fill is asymmetric, with thicker sedimentary and peat infill to the northeast (~100 m
145 thick; Domingo-García et al., 1983; Florschütz et al., 1971; Nestares and Torres, 1997) and
146 progressively becoming thinner to the southwest (Alfaro et al., 2001). The main source area
147 of allochthonous sediments in the bog is the Sierra Nevada, which is characterized at higher
148 elevations by Paleozoic siliceous metamorphic rocks (mostly mica-schists and quartzites)
149 from the Nevado-Filabride complex and, at lower elevations and acting as bedrock, by
150 Triassic dolomites, limestones and phyllites from the Alpujárride Complex (Sanz de
151 Galdeano et al. 1998). Geochemistry in the Padul sediments is influenced by detritic
152 materials also primarily from from the the Sierra Nevada (Ortiz et al., 2004). Groundwater
153 inputs into the Padul basin come from the Triassic carbonates aquifers (N and S edge to the
154 basin), the out flow of the Granada Basin (W edge to the basin) and the conglomerate aquifer
155 to the east edge (Castillo Martín et al., 1984; Ortiz et al., 2004). The main water output is by
156 evaporation and evapotranspiration, water wells and by canals ("madres") that drain the water
157 to the Dúrcal river to the southeast (Castillo Martín et al., 1984). Climate in the Padul area is
158 characterized by a mean annual temperature of 14.4 ºC and a mean annual precipitation of
159 445 mm (http://www.aemet.es/).
160 The Padul-15-05 drilling site was located ~50 m south of the present-day Padul lake shore
161 area. This basin area is presently subjected to seasonal water level fluctuations and is
162 principally dominated by *Phragmites australis* (Poaceae). The lake environment is dominated
163 by aquatic and wetland communities with *Chara vulgaris*, *Myriophyllum spicatum*,
164 *Potamogeton pectinatus*, *Potamogetum coloratus*, *Phragmites australis*, *Typha*
165 *dominguensis*, *Apium nodiflorum*, *Juncus subnodulosus*, *J. bufonius*, *Carex hispida and*
166 *Ranunculus muricatus*, among others (Pérez Raya and López Nieto, 1991). Some sparse
167 riparian trees occur in the northern lake shore, such as *Populus alba*, *Populus nigra*, *Salix* sp.,
168 *Ulmus minor* and *Tamarix*. At present *Phragmites australis* is the most abundant plant
169 bordering the lake. Surrounding this area are cultivated crops with cereals, such as *Triticum*
170 spp., as well as *Prunus dulcis* and *Olea europea*.

171 **3 Material and methods**

172 Two sediment cores, Padul-13-01 (37º00'40''N; 3º36'13''W) and Padul-15-05
173 (37º00'39.77''N; 3º36'14.06''W) with a length of 58.7 cm and 42.64 m, respectively, were
174 collected between 2013 and 2015 from the wetland (Fig. 1). The cores were taken using a
175 Rolatec RL-48-L drilling machine equipped with a hydraulic piston corer from the Scientific
176 Instrumentation Centre of the University of Granada (UGR). The sediment cores were
177 wrapped in film, put in core boxes, transported to UGR and stored in a dark cool room at 4ºC.

178 **3.1 Age-depth model (AMS radiocarbon dating)**

179 The core chronology was constrained using fourteen AMS radiocarbon dates from plant
180 remains and organic bulk samples taken from the cores (Table 1). In addition, one sample
181 with gastropods was also submitted for AMS radiocarbon analysis, although it was rejected
182 due to important reservoir effect, that provided a very old date. Thirteen of these samples
183 came from Padul-15-05 with one from the nearby Padul-13-01 (Table 1). We were able to
184 use this date from Padul-13-01 core as there is a very significant correlation between the
185 upper part of Padul-15-05 and Padul-13-01 cores, shown by identical lithological and
186 geochemical changes (Supplementary information 1; Figure S1). The age model for the upper
187 ~3 m minus the upper 21 cm from the surface was built using the R-code package 'Clam 2.2'

188 (Blaauw, 2010) employing the calibration curve IntCal 13 (Reimer et al., 2013), a 95 % of
189 confidence range, a smooth spline (type 4) with a 0.20 smoothing value and 1000 iterations
190 (Fig. 2). The chronology of the uppermost 21 cm of the record was built using a linear
191 interpolation between the last radiocarbon date and the top of the record (Present; 2015 CE).
192 Even though the length of the Padul-15-05 core is ~43 m, the studied interval in the work
193 presented here is the uppermost 115 cm of the record that are constrained by seven AMS
194 radiocarbon dates (Fig. 2).

195 **3.2 Lithology, MS, XRF and TOC**

196 Padul-15-05 core was split longitudinally and was described in the laboratory with respect to
197 lithology and color (Fig. 3). Magnetic susceptibility (MS) was measured with a Bartington
198 MS3 operating with a MS2E sensor. MS measurements (in SI units) were obtained directly
199 from the core surface every 0.5 cm (Fig. 3).
200
201 Elemental geochemical composition was measured in an X-Ray fluorescence (XRF)
202 Avaatech core scanner® at the University of Barcelona (Spain). A total of thirty-three
203 chemical elements were measured in the XRF core scanner at 10 mm of spatial resolution,
204 using 10 s count time, 10 kV X-ray voltage and a X-ray current of 650 μA for lighter
205 elements and 35 s count time, 30 kV X-ray voltage, X-ray current of 1700 μA for heavier
206 elements. Thirty-three chemical elements were measured but only the most representative
207 with a major number of counts were considered (Si, K, Ca, Ti, Fe, Zr, Br and Sr). Results for
208 each element are expressed as intensities in counts per second (cps) and normalized (norm.)
209 for the total sum in cps in every measure (Fig. 3).
210 Total organic carbon (TOC) was analyzed every 2 or 3 cm throughout the core. Samples were
211 previously decalcified with 1:1 HCl in order to eliminate the carbonate fraction. The
212 percentage of organic Carbon (OC %) was measured in an Elemental Analyzer Thermo
213 Scientific Flash 2000 model from the Scientific Instrumentation Centre of the UGR (Spain).
214 Percentage of TOC per gram of sediment was calculated from the percentage of organic
215 carbon (OC %) yielded by the elemental analyzer, and recalculated by the weight of the
216 sample prior to decalcification (Fig. 3).

217 **3.3 Pollen and NPP**

218 Samples for pollen analysis (1-3 cm^3) were taken every 1 cm throughout the core, with a total
219 of 103 samples analyzes. Pollen extraction methods followed a modified Faegri and Iversen
220 (1989) methodology. Processing included the addition of *Lycopodium* spores for calculation
221 of pollen concentration. Sediment was treated with NaOH, HCl, HF and the residue was
222 sieved at 250 μm previous to an acetolysis solution. Counting was performed using a
223 transmitted light microscope at 400 magnifications to an average pollen count of ca. 260
224 terrestrial pollen grains. Fossil pollen was identified using published keys (Beug, 2004) and
225 modern reference collections at University of Granada (Spain). Pollen counts were
226 transformed to pollen percentages based on the terrestrial pollen sum, excluding aquatics.
227 The palynological zonation was executed by cluster analysis using twelve primary pollen
228 taxa- *Olea*, *Pinus*, deciduous *Quercus*, evergreen *Quercus*, *Pistacia*, Ericaceae, *Artemisia*,
229 Asteroideae, Cichorioideae, Amaranthaceae and Poaceae (Grimm, 1987) (Fig. 4). Non-pollen
230 palynomorphs (NPP) include fungal and algal spores, and thecamoebians (testate amoebae).
231 The NPP percentages were calculated and represented with respect to the terrestrial pollen
232 sum (Fig. 4). Furthermore, some pollen taxa were grouped, according to present-day
233 ecological bases, into Mediterranean forest and xerophytes (Fig. 4). The Mediterranean forest

234 taxa is composed of *Quercus* total, *Olea*, *Phillyrea* and *Pistacia*. The xerophyte group
235 includes *Artemisia*, *Ephedra*, and Amaranthaceae.

4 Results

4.1 Chronology and sedimentation rates

238 The age-model of the upper 115 cm of Padul-15-05 core (Fig. 2) shows an average
239 sedimentation rate (SAR) of 0.058 cm/yr over last ~4700 cal yr BP, being the age constrained
240 by seven AMS ^{14}C dates (Table 1). However, SARs of individual core segments vary from
241 0.01 to 0.16 cm/yr (Fig. 2), showing the lowest values between ~51 and 40 cm (from ~2600
242 to 1350 cal yr BP) and the highest values during the last ~20 cm (last century).

4.2 Lithology, MS, XRF and TOC

244 The stratigraphy of the upper ~115 cm of the Padul-15-05 sediment core was deduced
245 primarily by visual inspection. However, our visual inspections were support by comparison
246 with the element geochemical composition (XRF), the MS of the split cores, and TOC (Fig.
247 3) to determine shifts in sediment facies. The lithology for this sedimentary sequence consists
248 in clays with variable carbonates, siliciclastics and organic content (Fig. 3). We also used a
249 Linear r (Pearson) correlation to calculated relationship for the XRF data. The correlation for
250 the inorganic geochemical elements determined two different groups of elements that covary
251 (Table 2): Group 1) Si, K, Ti, Fe and Zr with a high positive correlation between them;
252 Group 2) Ca, Br and Sr have negative correlation with Group 1. Based on this, the sequence
253 is subdivided in two principal sedimentary units. The lower ~87 cm of the record is
254 designated to Unit 1, characterized principally by relatively low values of MS and higher
255 values of Ca. The upper ~28 cm of the sequence is designated to Unit 2, in which the
256 mineralogical composition is lower in Ca with higher values of MS in correlation with mostly
257 siliciclastics elements (Si, K, Ti, Fe and Zr).
258
259 Within these two units, four different facies can be identified by visual inspection and by the
260 elemental geochemical composition and TOC of the sediments. *Facies* 1 (115-110 cm depth,
261 ~4700 to 4650 cal yr BP; and 89-80 cm depth ~4300 to 4000 cal yr BP) are characterized by
262 dark brown organic clays that bear charophytes and macroscopic plant remains. They also
263 have depicted relative higher values of TOC values (Fig. 3). *Facies* 2 (110-89 cm depth
264 ~4650 to 4300 cal yr BP; and 80-42 cm depth, ~4000 to 1600 cal yr BP) is compose of brown
265 clays, with the occurrence of gastropods and charophytes. This facies is also characterized by
266 lower TOC values. *Facies* 3 (42-28 cm depth, ~1600 to 400 cal yr BP) is characterized by
267 grayish brown clays with the occurrence of gastropods, and lower values of TOC, and an
268 increasing trend in MS and in siliciclastic elements. *Facies* 4 (28-0 cm, ~400 cal yr BP to
269 Present) is made up of light grayish brown clays and features a strong increase in siliciclastic
270 linked to a strong increase in MS.

4.3 Pollen and NPP

272 Several terrestrial and aquatic pollen taxa were identified but only the most representative
273 taxa are here plotted in the summary pollen diagram (Fig. 4). Selected NPP percentages are
274 also displayed in Figure 4. Four pollen zones (PA) were visually identified with the help of a
275 cluster analysis using the program CONISS (Grimm, 1987). Pollen concentration was higher
276 during Unit 1 with a decreasing trend in the transition to Unit 2 and a later increase during the
277 pollen subzone PA-4b (Fig. 4). Pollen zones are described below:

4.3.1 Zone PA-1 [~4720 to 3400 cal yr BP/ ~2800 to 1450 BCE (115-65 cm)]

Zone 1 is characterized by the abundance of Mediterranean forest species reaching up to ca. 70 %. Another important taxon in this zone is *Pinus,* with average values around 18 %. Herbs are largely represented by Poaceae, averaging around 10 %, and reaching up to ca. 25 %. This pollen zone is subdivided into PA-1a, PA-1b and PA-1c (Fig. 4). The principal characteristic that differentiating PA-1a from PA-1b (boundary at ~4650 cal yr BP/~2700 BCE) is the decrease in Poaceae, the increase in *Pinus*, and the appearance of cf. *Vitis.* The subsequent decrease in Mediterranean forest pollen to average values around 40 %, the increase in *Pinus* to average ~25 % and a progressive increase in Ericaceae to ~6 to 11 %, distinguishes subzones PA-1b and PA-1c (boundary at ca. 3950 cal yr BP).

4.3.2. Zone PA-2 [~3400 to 1550 cal yr BP/~1450 BCE to 400 CE (65-41 cm)]

The main features of this zone are the increase in Ericaceae up to ~16 %, some herbs such as Cichorioideae, became more abundant reaching average percentages of ~7 %. This pollen zone can be subdivided in subzones PA-2a and PA-2b with a boundary at ~2850 cal yr BP (~900 BCE). The principal characteristics that differentiate these subzones is marked by the increasing trend in Ericaceae and deciduous *Quercus* reaching maximum values of ~30 % and ~20 %, respectively. In addition, the increase in *Botryococcus,* which averages from ~4 to 9 %. Also notable is the expansion of *Mougeotia* and *Zygnema* types.

4.3.3 Zone PA-3 [~1550 to 400 cal yr BP/~400 CE to 1550 CE (41-29 cm)]

This zone is distinguished by the continuing decline of Mediterranean forest elements. Cichorioideae reached average values of about 40 %, and is paralleled by the decrease in Ericaceae. A decline in *Botryococcus* and other algal remains is also observed in this zone, although there is an increase in total Thecamoebians from average of <1 % to 10 %. This pollen zone is subdivided in subzones PA-3a and PA-3b at ~1000 cal yr BP (~950 CE). The main features that differentiate these subzones are the increase in *Olea* from subzone PA-3a to PA-3b from average values of ~1 to 5 %. The increasing trend in Poaceae is also a feature in this subzone, as well as the slight increase in Asteroideae at the top. Significant changes are documented in NPP percentages in this subzone with the increase of some fungal remain such as *Tilletia* and *Glomus* type. Furthermore, a decrease in *Botrycoccus* and the near disappearance of other algal remains such as *Mougetia* occurred.

4.3.4 Zone PA-4 [~last 400 cal yr BP/ ~ 1550 CE to Present (29-0 cm)]

The main feature in this zone is the significant increase in *Pinus,* reaching maximum values of ~32 %, an increase in Poaceae to ~40 %) and the decrease in Cichorioideae (~44 to 16 %). Other important changes are the nearly total disappearance of some shrubs such as *Pistacia* and a decreasing trend in Ericaceae, as well as a further decline in Mediterranean forest pollen. An increase in wetland pollen taxa, mostly *Typha*, also occurred. A significant increase in xerophytes, mostly Amaranthaceae to ~14 % is also observed in this period. Other herbs such as *Plantago*, Polygonaceae and Convolvulaceae show moderate increases. PA-4 is subdivided into subzones PA-4a and PA-4b (Fig. 4). The top of the record (PA-4b), which corresponds with the last ~120 yr, is differentiated from subzone PA-4a (from ~400 – 120 cal yr BP) by a decline in some herbs such as Cichorioideae. However, an increase in other herbs such as Amaranthaceae and Poaceae occurred. The increase in *Plantago* is also significant during this period. PA-4b also has a noteworthy increase in *Pinus* (from ~14 to 27 %) and a slight increase in *Olea* and evergreen *Quercus* are also characteristic of this subzone. With

322 respect to NPPs, thecamoebians such as *Arcella* type and in the largely coprophilous
323 sordariaceous (Sordariales) spores also increase. This zone also documents the decrease in
324 fresh-water algal spores, in *Botryococcus* concomitant with *Mougeotia and Zygnema type*.

4.4 Estimated lake level reconstruction

326 Different local proxies from the Padul-15-05 record [Si, Ca, TOC, MS, hygrophytes
327 (Cyperaceae and *Typha*), Poaceae and algae (including *Botryoccocus*, *Zygnema* types
328 and *Mougeotia*) groups] have been depicted in order to understand the relationship between
329 lithological, geochemical, and palynological variability and the water lake level oscillations.
330 Sediments with higher values of TOC (more algae and hygrophytes) and rich in Ca (related
331 with the occurrence of shells and charophytes remains) most likely characterized a shallow
332 water environment (Unit 1). The continuous decline in *Botryococcus*, the disappearance of
333 charophytes and the progressively increase in detritics (increase in MS and Si values) could
334 be associated with shallower and even ephemeral lake environment (transition from Unit 1 to
335 Unit 2; ~41 to 28 cm). The absence of aquatic remains, almost disappearance of
336 *Botryococcus* and decreasing Ca and a lower TOC and/or a higher input of clastic material
337 (higher MS and Si values) into the lake, could be related with lake level lowering, and even
338 emerged conditions (increase in Poaceae; Unit 2) (Fig. 5).

4.5 Spectral analysis

340 Spectral analysis was performed on selected pollen and NPP time series (Mediterranean
341 forest and *Botryococcus)*, as well as TOC in order to identify millennial- and centennial-scale
342 periodicities. The mean sampling resolution for pollen and NPP is ~50 yr and for
343 geochemical data is ~80 yr. Statistically significant cycles, above the 90, 95 and 99 % of
344 confident levels, were found around 800, 680, 300, 240, 200, 170 (Fig. 7).

5 Discussion

346 Numerous proxies have been used in this study to interpret the paleoenvironmental and
347 hydrodynamic changes recorded in the Padul sedimentary record during the last 4700 cal yr
348 BP. Palynological analysis (pollen and NPP) is commonly used as a proxy for vegetation and
349 climate change, and lake level variations, as well as human impact and land uses (e.g. Faegri
350 and Iversen, 1990; van Geel et al., 1983). Disentangling natural vs. anthropogenic effects on
351 the environment in the last millennials is sometimes challenging but can be persuaded using a
352 multi-proxy approach (Roberts et al., 2011; Sadori et al., 2011). In this study, we used the
353 variations between Mediterranean forest taxa, xerophytes and algal communities for
354 paleoclimatic variability and the occurrence of nitrophilous and ruderal plant communities
355 and some NPPs for identifying human influence in the study area. Variations in arboreal
356 pollen (AP, including Mediterranean tree species) have previously been used in previous
357 Sierra Nevada records as a proxy for humidity changes (Jiménez-Moreno and Anderson,
358 2012; Ramos-Román et al., 2016). The increase or decrease in Mediterranean forest species
359 has been used as a proxy for climate change in other studies in the western Mediterranean
360 region, with greater forest development generally meaning higher humidity (Fletcher et al.,
361 2013; Fletcher and Sánchez-Goñi, 2008). On the other hand, increases in xerophyte pollen
362 taxa (i.e., *Artemisia*, *Ephedra*, Amaranthaceae) have been used as an indication of aridity in
363 this area (Anderson et al., 2011; Carrión et al., 2007).

365 The chlorophyceae alga *Botryococcus* sp. has been used as an indicator of freshwater
366 environments, in relatively productive fens, temporary pools, ponds or lakes (Guy-Ohlson,

367   1992). The high visual and statistical correlation between *Botryococcus* from Padul-15-05
368   and North Atlantic temperature estimations [Bond et al., 2001; r = -0.63; *p* < 0.0001; between
369   ca. 4700 to 1500 cal yr BP and r=-0.48; *p* < 0.0001 between 4700 and -65 cal yr BP (the
370   decreasing and very low *Botryococcus* occurrence in the last 1500 cal yr BP makes this
371   correlation moderate)] seems to show that in this case *Botryococcus* is driven by temperature
372   change and would reflect variations in lake productivity (increasing with warmer water
373   temperatures).

374

375   Human impact can be investigated using several palynomorphs. Nitrophilous and ruderal
376   pollen taxa, such as *Convolvulus*, *Plantago lanceolata* type, Urticaceae type and *Polygonum*
377   *avicularis* type, are often proxies for human impact (Riera et al., 2004), and abundant
378   Amaranthaceae has also been used as well (Sadori et al., 2003). Some species of
379   Cichorioideae have been described as nitrophilous taxa (Abel-Schaad and López-Sáez, 2013)
380   and as grazing indicators (Florenzano et al., 2015; Mercuri et al., 2006; Sadori et al., 2016).
381   At the same time, NPP taxa such as some coprophilous fungi, Sordariales and thecamoebians
382   are also used as indicators of anthropization and land use (Carrión et al., 2007; Ejarque et al.,
383   2015; van Geel et al., 1989; Riera et al., 2006). *Tilletia* a grass-parasitizing fungi has been
384   described as an indicator of grass cultivation in other Iberian records (Carrión et al., 2001a).
385   In this study we follow the example of others (van Geel et al., 1989; Morellón et al., 2016;
386   Sadori et al., 2016) who used the NPP soil mycorrhizal fungus *Glomus* sp. as a proxy for
387   erosive activity.

388

389   The palynological analysis, variations in the lithology, geochemistry and macrofossil remains
390   (gastropod shells and charophytes) from the Padul-15-05 core helped us reconstruct the
391   estimated lake level and the local environment changes in the Padul area and their
392   relationship with regional climate (Fig. 5). Several previous studies on Late Holocene lake
393   records from the Iberian Peninsula show that lithological changes can be used as a proxy for
394   lake level reconstruction (Martín-Puertas et al., 2011; Morellón et al., 2009; Riera et al.,
395   2004). For example, carbonate sediments formed by biogenic remains of gastropods and
396   charophytes are indicative of shallow lake waters (Riera et al., 2004). Furthermore, van Geel
397   et al. (1983), described occurrences of *Mougeotia* and *Zygnema* type (Zygnemataceae) as
398   typical of shallow water environments. The increase in organic matter accumulation deduced
399   by TOC (and Br) could be considered as characteristic of high productivity (Kalugin et al.,
400   2007) in these shallow water environments. On the other hand, increases in clastic input in
401   lake sediments have been interpreted as due to lowering of lake level and more influence of
402   terrestrial-fluvial deposition in a very shallow/ephemeral lake (Martín-Puertas et al., 2008).
403   Carrión (2002) related the increase in some fungal species and Asteraceae as indicators of
404   seasonal desiccation stages in lakes. Nevertheless, in natural environments with potential
405   interactions with human activities the increase in clastic deposition related with other
406   indications of soil erosion (e.g. *Glomus* sp.) may be assigned to intensification in land use
407   (Morellón et al., 2016; Sadori et al., 2016).

408   **5.1 Late Holocene aridification trend**

409   Our work confirms the progressive aridification trend that occurred during at least the last
410   ~4700 cal yr BP in the southern Iberian Peninsula, as shown here by the progressive decrease
411   in Mediterranean forest component and the increase in herbs (Figs. 4 and 6). Our lake level
412   interpretations agree with the pollen data, showing an overall decrease during the Late
413   Holocene, from a shallow water table containing relatively abundant organic matter (high
414   TOC, indicating higher productivity), gastropods and charophytes (high Ca values) to a low-

415 productive ephemeral/emerged environment (high clastic input and MS and decrease in Ca)
416 (Fig. 5). This natural progressive aridification confirmed by the decrease in Mediterranean
417 forest taxa and increase in siliciclastics pointing to a change towards ephemeral (even
418 emerged) environments became more prominent since about 1550 cal yr BP and then
419 enhanced again since ca. 400 cal yr BP to Present. A clear increase in human land use is also
420 observed during the last ca. 1550 cal yr BP (see bellow), including abundant *Glomus* from
421 erosion, which shows that humans were at least partially responsible for this sedimentary
422 change.
423
424 A suite of proxies previous studies supports our conclusions regarding the aridification trend
425 since the Middle Holocene (Carrión, 2002; Carrión et al., 2010; Fletcher et al., 2013; Fletcher
426 and Sánchez-Goñi, 2008; Jiménez-Espejo et al., 2014; Jiménez-Moreno et al., 2015). In the
427 western Mediterranean region the decline in forest development during the Middle and Late
428 Holocene is related with a decrease in summer insolation (Fletcher et al., 2013; Jiménez-
429 Moreno and Anderson, 2012), which may have decreased winter rainfall as a consequence of
430 a northward shift of the westerlies - a long-term enhanced positive NAO trend – which
431 induced drier conditions in this area since 6000 cal yr BP (Magny et al., 2012). Furthermore,
432 the decrease in summer insolation would produce a progressive cooling, with a reduction in
433 the length of the growing season as well as a decrease in the sea-surface temperature
434 (Marchal et al., 2002), generating a decrease in the land-sea contrast that would be reflected
435 in a reduction of the wind system and a reduced precipitation gradient from sea to shore
436 during the fall-winter season. The aridification trend can clearly be seen in the nearby alpine
437 records from the Sierra Nevada, where there was little influence by human activity (Anderson
438 et al., 2011; Jiménez-Moreno et al., 2013; Jiménez-Moreno and Anderson, 2012; Ramos-
439 Román et al., 2016).
440

441 **5.2 Millennial- and centennial-scale climate variability in the Padul area during the**
442 **Late Holocene**

443 The multi-proxy paleoclimate record from Padul-15-05 shows an overall aridification trend.
444 However, this trend seems to be modulated by millennial- and centennial-scale climatic
445 variability.

446 **5.2.1 Aridity pulses around 4200 (4500, 4300 and 4000 cal yr BP) and around 3000 cal**
447 **yr BP (3300 and 2800 cal yr BP)**

448 Marked aridity pulses are registered in the Padul-15-05 record around 4200 and 3000 cal yr
449 BP (Unit 1; PA-1 an PA-2a; Figs. 5 and 6). These arid pulses are mostly evidenced in this
450 record by declines in Mediterranean forest taxa, as well as lake level drops and/or cooling
451 evidenced by a decrease in organic component as TOC and the decrease in *Botryococcus*
452 algae. However, a discrepancy between the local and regional occurs between 3000-2800 cal
453 yr BP, with an increase in the estimated lake level and a decrease in the Mediterranean forest
454 during the late Bronze Age until the early Iron Age (Figs. 5 and 6). The disagreement could
455 be due to deforestation by humans during a very active period of mining in the area observed
456 as a peak in lead pollution in the alpine records from Sierra Nevada (García-Alix et al.,
457 2013). The aridity pulses agree regionally with recent studies carried out at higher in
458 elevation in the Sierra Nevada, a decrease in AP percentage in Borreguil de la Caldera record
459 around 4000-3500 cal yr BP (Ramos-Román et al., 2016), high percentage of non-arboreal
460 pollen around 3400 cal ka BP in Zoñar lake [Southern Córdoba Natural Reserve; (Martín-
461 Puertas et al., 2008)], and lake desiccation at ca. 4100 and 2900 cal yr BP in Lake Siles

462 (Carrión et al., 2007). Jalut et al. (2009) compared paleoclimatic records from different lakes
463 in the western Mediterranean region and also suggested a dry phase between 4300 to 3400 cal
464 yr BP, synchronous with this aridification phase. Furthermore, in the eastern Mediterranean
465 basin other pollen studies show a decrease in arboreal pollen concentration toward more open
466 landscapes around 4 cal ka BP (Magri, 1999).
467
468 Significant climatic changes also occurred in the Northern Hemisphere at those times and
469 polar cooling and tropical aridity are observed at ~4200-3800 and 3500-2500 cal yr BP;
470 (Mayewski et al., 2004), cold events in the North Atlantic [cold event 3 and 2; (Bond et al.,
471 2001)], decrease in solar irradiance (Steinhilber et al., 2009) and humidity decreases in the
472 eastern Mediterranean area at 4200 cal yr BP (Bar-Matthews et al., 2003) that could be
473 related with global scale climate variability (Fig. 6). These generally dry phases between 4.5
474 and 2.8 in Padul-15-05 are generally in agreement with persistent positive NAO conditions
475 during this time (Olsen et al., 2012).
476 The high-resolution Padul-15-05 record shows that climatic crises such as the essentially
477 global event at~4200 cal yr BP (Booth et al., 2005), are actually multiple events in climate
478 variability at centennial-scales (i.e., ca. 4500, 4300, 4000 cal yr BP).

479 **5.2.2 Iberian-Roman Humid Period (~2600 to 1600 cal yr BP)**

480 High relative humidity is recorded in the Padul-15-05 record between ~2600 and 1600 cal yr
481 BP, synchronous with the well-known Iberian-Roman Humid Period (IRHP; between 2600
482 and 1600 cal yr BP; (Martín-Puertas et al., 2009). This is interpreted in our record due to an
483 increase in the Mediterranean forest species at that time (Unit 1; PA-2b; Figs. 6). In addition,
484 there is a simultaneous increase in *Botryococcus* algae, which is probably related to higher
485 productivity during warmer conditions and relatively higher water level. A minimum in
486 sedimentary rates at this time is also recorded, probably related with lower detritic input
487 caused by less erosion due to afforestation and probably also related to the decrease in TOC
488 due to less organic accumulation in the sediment. Evidence of a wetter climate around this
489 period has also been shown in several alpine records from Sierra Nevada. For example, in the
490 Laguna de la Mula core (Jiménez-Moreno et al. 2013) an increase in deciduous *Quercus* is
491 correlated with the maximum in algae between 2500 to 1850 cal yr BP, also evidencing the
492 most humid period of the Late Holocene. A geochemical study from the Laguna de Río Seco
493 (also in Sierra Nevada) also evidenced humid conditions around 2200 cal yr BP by the
494 decrease in Saharan dust input and the increase in detritic sedimentation into the lake
495 suggesting higher rainfall (Jiménez-Espejo et al., 2014). In addition, Ramos-Román et al.
496 (2016) showed an increase in AP in the Borreguil de la Caldera record around 2200 cal yr
497 BP, suggesting an increase in humidity at that time.
498
499 Other records from the Iberian Peninsula also show this pattern to wetter conditions during
500 the IRHP. For example, high lake levels are recorded in Zoñar Lake in southern Spain
501 between 2460 to 1600 cal yr BP, only interrupted by a relatively arid pulse between 2140 and
502 1800 cal yr BP (Martín-Puertas et al., 2009). An increase in rainfall is described in the central
503 region of the Iberian Peninsula in a study from the Tablas de Daimiel National Park between
504 2100 and 1680 cal yr BP (Gil García et al., 2007). Deeper lake levels at around 2650 to 1580
505 cal yr BP, also interrupted by an short arid event at ca. 2125-1790 cal yr BP, were observed
506 to the north, in the Iberian Range (Currás et al., 2012). The fact that the Padul-15-05 record
507 also shows a relatively arid-cold event between 2150-2050 cal yr BP, just in the middle of
508 this relative humid-warm period, seems to point to a common feature of centennial-scale
509 climatic variability in many western Mediterranean and North Atlantic records (Fig. 6).

510 Humid climate conditions at around 2500 cal yr BP are also interpreted in previous studies
511 from lake level reconstructions from Central Europe (Magny, 2004). Increases in temperate
512 deciduous forest are also observed in marine records from the Alboran Sea around 2600 to
513 2300 cal yr BP, also pointing to high relative humidity (Combourieu-Nebout et al., 2009).
514 Overall humid conditions between 2600 and 1600 cal yr BP seem to agree with predominant
515 negative NAO reconstructions at that time, which would translate into greater winter (and
516 thus more effective) precipitation in the area triggering greater development of forest species
517 in the area.
518
519 Generally warm conditions are interpreted between 1900 and 1700 cal yr BP in the
520 Mediterranean Sea, with high sea surface temperatures (SSTs), and in the North Atlantic
521 area, with the decrease in Drift Ice Index. In addition, persistent positive solar irradiance
522 occurred at that time. The increase in *Botryococcus* algae reaching maxima during the IRHP
523 also seems to point to very productive and perhaps warmer conditions in the Padul area (Fig.
524 6). There seems to be a short lag of about 200 years between maximum in *Botryococcus* and
525 maximum in Mediterranean forest. This could be due to different speed of reaction to climate
526 change, with algae (short life cycle, blooming if conditions are favorable) responding faster
527 than forest (tree development takes decades). An alternative explanation could be that they
528 might be responding to different forcings, with regional signal (forest) mostly conditioned by
529 precipitation and local (algae) also conditioned by temperature (productivity).

530 **5.2.3 DA and MCA (~1550 cal yr BP to 600 cal yr BP)**

531 Enhanced aridity occurred right after the IRHP in the Padul area. This is deduced in the
532 Padul-15-05 record by a significant forest decline, with a prominent decrease in
533 Mediterranean forest elements, an increase in herbs (Unit 1; PA-3; Figs. 4 and 6). In addition,
534 our evidence suggests a transition from a shallow lake to a more ephemeral wetland. This is
535 suggested by the disappearance of charophytes, a significant decrease in algae component
536 and higher Si and MS and lower TOC values (Unit 1; Figs. 5). Humans probably also
537 contributed to enhancing erosion in the area during this last ~1550 cal yr BP. The significant
538 change during the transition from Unit 1 to Unit 2 with a decrease in the pollen concentration
539 and the increase in Cichoroideae could be due to enhanced pollen degradation as
540 Cichoroideae have been found to be very resistant to pollen deterioration (Bottema, 1975).
541 However, the occurrence of other pollen taxa (e.g. *Quercus*, Ericaceae, *Pinus*, Poaceae, *Olea*)
542 showing climatic trends and increasing between ca. 1500-400 cal yr BP and a decrease in
543 Cichoroideae in the last ~400 cal yr BP, when an increase in clastic material occurred, do not
544 entirely support a preservation issue (see section of Human activity; 5.4).
545
546 This phase could be separated into two different periods. The first period occurred between
547 ~1550 cal yr BP and 1100 cal yr BP (~400 to 900 CE) and is characterized by a decreasing
548 trend in Mediterranean forest and *Botryococcus* taxa. This period corresponds with the Dark
549 Ages [from ca. 500 to 900 CE; (Moreno et al., 2012)]. Correlation between the decline in
550 Mediterranean forest, the increase in the Drift Ice Index in the North Atlantic record (cold
551 event 1; Bond et al., 2001), the decline in SSTs in the Mediterranean Sea and maxima in
552 positive NAO reconstructions suggests drier and colder conditions during this time (Fig. 6).
553 Other Mediterranean and central-European records agree with our climate interpretations, for
554 example, a decrease in forest pollen types is shown in a marine record from the Alboran Sea
555 (Fletcher et al., 2013) and a decrease in lake levels is also observed in Central Europe
556 (Magny et a., 2004) pointing to aridity during the DA. Evidences of aridity during the DA
557 have been shown too in the Mediterranean part of the Iberian Peninsula, for instance, cold

558 and arid conditions were suggested in the northern Betic Range by the increase in xerophytic
559 herbs around 1450 and 750 cal yr BP (Carrión et al., 2001b) and in southeastern Spain by a
560 forest decline in lacustrine deposits around 1620 and 1160 cal yr BP (Carrión et al., 2003).
561 Arid and colder conditions during the Dark Ages (around 1680 to 1000 cal yr BP) are also
562 suggested for the central part of the Iberian Peninsula using a multiproxy study of a sediment
563 record from the Tablas de Daimiel Lake (Gil García et al., 2007).
564
565 A second period that we could differentiate occurred around 1100 to 600 cal yr BP/900 to
566 1350 CE, during the well-known MCA (900 to 1300 CE after Moreno et al., 2012). During
567 this period the Padul-15-05 record shows a slight increasing trend in the Mediterranean forest
568 taxa with respect to the DA, but the decrease in *Botryococcus* and the increase in herbs still
569 point to overall arid conditions. This change could be related to an increase in temperature,
570 favoring the development of temperate forest species, and would agree with inferred
571 increasing temperatures in the North Atlantic areas, as well as the increase in solar irradiance
572 and the increase in SSTs in the Mediterranean Sea (Fig. 6). This hypothesis would agree with
573 the reconstruction of persistent positive NAO and overall warm conditions during the MCA
574 in the western Mediterranean (see synthesis in Moreno et al., 2012). A similar pattern of
575 increasing xerophytic vegetation during the MCA is observed in alpine peat bogs and lakes in
576 the Sierra Nevada (Anderson et al., 2011; Jiménez-Moreno et al., 2013; Ramos-Román et al.,
577 2016) and arid conditions are shown to occur during the MCA in southern and eastern Iberian
578 Peninsula deduced by increases in salinity and lower lake levels (Corella et al., 2013; Martín-
579 Puertas et al., 2011). However, humid conditions have been reconstructed for the
580 northwestern of the Iberian Peninsula at this time (Lebreiro et al., 2006; Moreno et al., 2012),
581 as well as northern Europe (Martín-Puertas et al., 2008). The different pattern of precipitation
582 between northwestern Iberia / northern Europe and the Mediterranean area is undoubtedly a
583 function of the NAO precipitation dipole (Trouet et al., 2009).

584 **5.2.4 The last ~600 cal yr BP: LIA (~600 to 100 cal yr BP/~1350 to1850 CE) and IE**
585 **(~100 cal yr BP to Present/~1850 CE-Present)**

586 Two climatically distinct periods can be distinguished during the last ~600 years (end of PA-
587 3b to PA-4; Fig. 4) in the area. However, the climatic signal is more difficult to interpret due
588 to a higher human impact at that time. The first phase around 600-500 cal yr BP was
589 characterized as increasing relative humidity by the decrease in xerophytes and the increase
590 in Mediterranean forest taxa and *Botryococcus* after a period of decrease during the DA and
591 MCA, corresponding to the LIA. The second phase is characterized here by the decrease in
592 the Mediterranean forest around 300-100 cal yr BP, pointing to a return to more arid
593 conditions during the last part of the LIA (Figs. 5 and 6). This climatic pattern agrees with an
594 increase in precipitation by the transition from positive to negative NAO mode and from
595 warmer to cooler conditions in the North Atlantic area during the first phase of the LIA and a
596 second phase characterized by cooler (cold event 0; Bond et al., 2001) and drier conditions
597 (Fig. 6). A stronger variability in the SSTs is described in the Mediterranean Sea during the
598 LIA (Fig. 6). Mayewski et al. (2004) described a period of climate variability during the
599 Holocene at this time (600 to 150 cal yr BP) suggesting a polar cooling but more humid in
600 some parts of the tropics. Regionally, (Morellón et al., 2011) also described a phase of more
601 humid conditions between 1530 to 1750 CE (420 to 200 cal yr BP) in a lake sediment record
602 from NE Spain. An alternation between wetter to drier periods during the LIA are also shown
603 in the nearby alpine record from Borreguil de la Caldera in the Sierra Nevada mountain range
604 (Ramos-Román et al., 2016).
605 The environmental transition from ephemeral, observed in the last ca. 1550 cal yr BP (Unit 1;

606 Fig. 5), to emerged conditions occur in the last ca. 400 cal yr BP. This is shown by the
607 highest MS and Si values, enhance sedimentation rates and the increase in wetland plants and
608 the stronger decrease in Ca and organic components (TOC) in the sediments in the uppermost
609 part of the Padul-15-05 record (Unit 2; Figs. 3 and 5).

610 **5.3 Centennial-scale variability**

611 Time series analysis has become important in determining the recurrent periodicity of
612 cyclical oscillations in paleoenvironmental sequences (e.g. Jiménez-Espejo et al., 2014;
613 Ramos-Román et al., 2016; Rodrigo-Gámiz et al., 2014; Fletcher et al., 2013). This analysis
614 also assists in understanding possible relationships between the paleoenvironmental proxy
615 data and the potential triggers of the observed cyclical changes: i.e., solar activity,
616 atmospheric, oceanic dynamics and climate evolution during the Holocene. The
617 cyclostratigraphic analysis on the pollen (Mediterranean forest; regional signal), algae
618 (*Botryococcus*; local signal) and TOC (local signal) times series from the Padul-15-05 record
619 evidence centennial-scale cyclical patterns with periodicities around ~800, 680, 300, 240, 200
620 and 170 years above the 90 % confidence levels (Fig. 7).

622 Previous cyclostratigraphic analysis in Holocene western Mediterranean records suggest
623 cyclical climatic oscillations with periodicities around 1500 and 1750 yr (Fletcher et al.,
624 2013; Jiménez-Espejo et al., 2014; Rodrigo-Gámiz et al., 2014). Other North Atlantic and
625 Mediterranean records also present cyclicities in their paleoclimatic proxies of ca. 1600 yr
626 (Bond et al., 2001; Debret et al., 2007; Rodrigo-Gámiz et al., 2014). However, this cycle is
627 absent from the cyclostratigraphic analysis in the Padul-15-05 record (Fig. 7). In contrast, the
628 spectral analysis performed in the Mediterranean forest time series from Padul record,
629 pointing to cyclical hydrological changes, shows a significant ~800 yr cycle that could be
630 related to solar variability (Damon and Sonett, 1991) or could be the second harmonic of the
631 ca. ~1600 yr oceanic-related cycle (Debret et al., 2009). A very similar periodicity of ca. 760
632 yr is detected in the *Pinus* forest taxa, also pointing to humidity variability, from the alpine
633 Sierra Nevada site of Borreguil de la Caldera and seems to show that this is a common
634 feature of cyclical paleoclimatic oscillation in the area.

636 A significant ~680 cycle is shown in the *Botryococcus* time series most likely suggesting
637 recurrent centennial-scale changes in temperature (productivity) and water availability. A
638 similar cycle is shown in the *Artemisia* signal in an alpine record from Sierra Nevada
639 (Ramos-Román et al., 2016). This cycle around ~650 yr is also observed in a marine record
640 from the Alboran Sea, and was interpreted as the secondary harmonic of the 1300 yr cycle
641 that those authors related with cyclic thermohaline circulation and sea surface temperature
642 changes (Rodrigo-Gámiz et al., 2014).

644 A statistically significant ~300 yr cycle is shown in the Mediterranean forest taxa and TOC
645 from the Padul-15-05 record suggesting shorter-scale variability in water availability. This
646 cycle is also observed in the cyclical *Pinus* pollen data from Borreguil de la Caldera at higher
647 elevations in the Sierra Nevada (Ramos-Román et al., 2016). This cycle could be principally
648 related to NAO variability as observed by Olsen et al. (2012), which follows variations in
649 humidity observed in the Padul-15-05 record. NAO variability also regulates modern
650 precipitation in the area.

652 The *Botryococcus* and TOC time series shows variability with a periodicity around ~240, 200
653 and 164 yrs. Sonett and Suess, (1984) described a significant cycle in solar activity around

654 ~208 yr (Suess solar cycle), which could have triggered our ~200 cyclicity. The observed
655 ~240 yr periodicity in the Padul-15-05 record could be either related to variations in solar
656 activity or due to the mixed effect of the solar together with the ~300 yr NAO-interpreted
657 cycle and could point to a solar origin of the centennial-scale NAO variations as suggested by
658 previously published research (Lukianova and Alekseev, 2004; Zanchettin et al., 2008).
659 Finally, a significant ~170 yr cycle has been observed in both the Mediterranean forest taxa
660 and *Botryococcus* times series from the Padul-15-05 record. A similar cycle (between 168-
661 174 yr) was also described in the alpine pollen record from Borreguil de la Caldera in Sierra
662 Nevada (Ramos-Román et al., 2016), which shows that it is a significant cyclical pattern in
663 climate, probably precipitation, in the area. This cycle could be related to the previously
664 described ~170 yr cycle in the NAO index (Olsen et al., 2012), which would agree with the
665 hypothesis of the NAO controlling millennial- and centennial-scale environmental variability
666 during the Late Holocene in the area (García-Alix et al., 2017; Ramos-Román et al., 2016).

667 **5.4 Human activity**

668 Humans probably had an impact in the area since Prehistoric times, however, the Padul-15-05
669 multiproxy record shows a more significant human impact during the last ca. 1550 cal yr BP,
670 which intensified in the last ~500 years (since 1450 CE to Present). This is deduced by, a
671 significant increase in nitrophilous plant taxa such as Cichorioideae, Convolvulaceae,
672 Polygonaceae and *Plantago* and the increase in some NPP such as *Tilletia*, coprophilous
673 fungi and thecamoebians (Unit 2; PA-4; Fig. 4). Most of these pollen taxa and NPPs are
674 described in other southern Iberian paleoenvironmental records as indicators of land uses, for
675 instance, *Tilletia* and covarying nitrophilous plants have been described as indicators of
676 farming (e.g. Carrión et al., 2001a). Thecamoebians also show a similar trend and have also
677 been detected in other areas being related to nutrient enrichment as consequences of livestock
678 (Fig. 8). The stronger increase in Cichorioideae have also been described as indicators of
679 animal grazing in areas subjected to intense use of the territory (Mercuri et al., 2006).
680 Interestingly, these taxa began to decline around ca. 400 cal yr BP (~1550 CE), coinciding
681 with the higher increase in detritic material into the basin. We could then interpreted this
682 increase in Cichorioideae as greater in livestock activity in the surroundings of the lake
683 during this period, which is supported by the increase in these other proxies related with
684 animal husbandry.

686 Climatically, this event coincides with the start of persistent negative NAO conditions in the
687 area (Trouet et al., 2009), which could have further triggered more rainfall and more detritic
688 input into the basin. Bellin et al., (2011) in a study from the Betic Cordillera (southern Iberian
689 Peninsula) demonstrate that soil erosion increase in years with higher rainfall and this could
690 be intensified by human impact. Nevertheless, in a study in the southeastern part of the
691 Iberian Peninsula (Bellin et al., 2013) suggested that major soil erosion could have occurred
692 by the abandonment of agricultural activities in the mountain areas as well as the
693 abandonment of irrigated terrace systems during the Christian Reconquest. Enhanced soil
694 erosion at this time is also supported by the increase in *Glomus* type (Figs. 4 and 8).

696 An important change in the sedimentation in the environment is observed during the last ca.
697 400 cal yr BP marked by the stronger increase in MS and Si values. This higher increase in
698 detritics occurred during an increase in other plants related with human and land uses such as
699 Polygonaceae, Amaranthaceae, Convolvulaceae, *Plantago*, Apiaceae and Cannabaceae-
700 Urticaceae type (Land Use Plants; Fig. 8). This was probably related to drainage canals in the
701 Padul wetland in the late XVIII century for cultivation purposes (Villegas Molina, 1967). The

increase in wetland vegetation and higher values of Poaceae could be due to cultivation of cereals or by an increase in the population of *Phragmites australis* (also a Poaceae), very abundant in the Padul lake margins at present due to the increase in drained land surface.

The uppermost part (last ca. 100 cal yr BP) of the pollen record from Padul-15-05 shows an increasing trend in some arboreal taxa at that time, including Mediterranean forest, *Olea* and *Pinus* (Fig. 4). This change is most likely of human origin and generated by the increase in *Olea* cultivation in the last two centuries, also observed in many records from higher elevation sites from Sierra Nevada, and *Pinus* and other Mediterranean species reforestation in the 20th century (Anderson et al., 2011; Jiménez-Moreno and Anderson, 2012; Jiménez-Moreno et al., 2013; Ramos-Román et al., 2016). Preliminary charcoal data show maxima in charcoal particle sedimentation coinciding with maxima in forest (fuel) during the Early and Middle Holocene humid and warmest maxima and do not show any increase in the last millennia, supporting our conclusions about little human impact in the area until very recent (Webster, pers. comm.). This agrees with previous studies on the area showing that Mediterranean fire regimes today are mostly conditioned by fuel load variations (Jiménez-Moreno et al., 2013; Ramos-Román et al., 2016).

6 Conclusions

Our multiproxy analysis from the Padul-15-05 sequence has provided a detailed climate reconstruction for the last 4700 ca yr BP for the Padul area and the western Mediterranean. This study, supported by the comparison with other Mediterranean and North Atlantic records suggests a link between vegetation, atmospheric dynamics and insolation and solar activity during the Late Holocene. A climatic aridification trend occurred during the Late Holocene in the Sierra Nevada and the western Mediterranean, probably linked with an orbital-scale declining trend in summer insolation. This long-term trend is modulated by centennial-scale climate variability as shown by the pollen (Mediterranean forest taxa), algae (*Botryococcus*) and sedimentary and geochemical data in the Padul record. These events can be correlated with regional and global scale climate variability. Cold and arid pulses identified in this study around the 4200 and 3000 cal yr BP are synchronous with cold events recorded in the North Atlantic and decreases in precipitation in the Mediterranean area, probably linked to persistent positive NAO mode. Moreover, one of the most important humid and warmer periods during the Late Holocene in the Padul area coincides in time with the well-known IRHP, characterized by warm and humid conditions in the Mediterranean and North Atlantic regions and overall negative NAO conditions. A drastic decline in Mediterranean forest taxa, trending towards an open landscape and pointing to colder conditions with enhanced aridity, occurred in two steps (DA and end of the LIA) during the last ~1550 cal yr BP. However, this trend was slightly superimposed by a more arid but warmer event coinciding with the MCA and a cold but wetter event during the first part of the LIA. Besides natural climatic and environmental variability, strong evidences exists for intense human activities in the area during the last ~1550 years. This suggests that the natural aridification trend during the Late Holocene, which produced a progressive decrease in the Mediterranean forest taxa in the Padul area, could have been intensified by human activities, notably in the last centuries.

Furthermore, time series analyses done in the Padul-15-05 record show centennial-scale changes in the environment and climate that are coincident with the periodicities observed in solar, oceanic and NAO reconstructions and could show a close cause-and-effect linkage between them.

Acknowledgements

This work was supported by the project P11-RNM-7332 funded by Consejería de Economía, Innovación, Ciencia y Empleo de la Junta de Andalucía, the project CGL2013-47038-R funded by Ministerio de Economía y Competitividad of Spain and fondo Europeo de desarrollo regional FEDER and the research group RNM0190 (Junta de Andalucía). M. J. R.-R. acknowledges the PhD funding provided by Consejería de Economía, Innovación, Ciencia y Empleo de la Junta de Andalucía (P11-RNM-7332). J.C. acknowledges the PhD funding provided by Ministerio de Economía y Competitividad (CGL2013-47038-R). A.G.-A. was also supported by a Ramón y Cajal Fellowship RYC-2015-18966 of the Spanish Government (Ministerio de Economía y Competividad). Javier Jaimez (CIC-UGR) is thanked for graciously helping with the coring, the drilling equipment and logistics. We also would like to thanks to Graciela Gil-Romera, Laura Sadori and an anonymous reviewer for their comments and suggestions which improved the manuscript.

762 **References**

763 Abel-Schaad, D. and López-Sáez, J. A.: Vegetation changes in relation to fire history and
764 human activities at the Peña Negra mire (Bejar Range, Iberian Central Mountain System,
765 Spain) during the past 4,000 years, Veg. Hist. Archaeobotany, 22(3), 199–214,
766 doi:10.1007/s00334-012-0368-9, 2013.

767 Alfaro, P., Galinod-Zaldievar, J., Jabaloy, A., López-Garrido, A. C. and Sanz de Galdeano,
768 C.: Evidence for the activity and paleoseismicity of the Padul fault (Betic Cordillera,
769 Southern Spain) [Evidencias de actividad y paleosismicidad de la falla de Padul (Cordillera
770 Bética, sur de España)], Acta Geol. Hisp., 36(3–4), 283–297, 2001.

771 Alpert, P., Baldi, M., Ilani, R., Krichak, S., Price, C., Rodó, X., Saaroni, H., Ziv, B., Kishcha,
772 P., Barkan, J., Mariotti, A. and Xoplaki, E.: Chapter 2 Relations between climate variability
773 in the Mediterranean region and the tropics: ENSO, South Asian and African monsoons,
774 hurricanes and Saharan dust, Dev. Earth Environ. Sci., 4(C), 149–177, doi:10.1016/S1571-
775 9197(06)80005-4, 2006.

776 Anderson, R. S., Jiménez-Moreno, G., Carrión, J. S. and Pérez-Martínez, C.: Postglacial
777 history of alpine vegetation, fire, and climate from Laguna de Río Seco, Sierra Nevada,
778 southern Spain, Quat. Sci. Rev., 30(13–14), 1615–1629,
779 doi:https://doi.org/10.1016/j.quascirev.2011.03.005, 2011.

780 Bar-Matthews, M., Ayalon, A., Gilmour, M., Matthews, A. and Hawkesworth, C. J.: Sea–
781 land oxygen isotopic relationships from planktonic foraminifera and speleothems in the
782 Eastern Mediterranean region and their implication for paleorainfall during interglacial
783 intervals, Geochim. Cosmochim. Acta, 67(17), 3181–3199,
784 doi:https://doi.org/10.1016/S0016-7037(02)01031-1, 2003.

785 Bellin, N., Vanacker, V., van Wesemael, B., Solé-Benet, A. and Bakker, M. M.: Natural and
786 anthropogenic controls on soil erosion in the internal betic Cordillera (southeast Spain),
787 Catena, 87(2), 190–200, doi:10.1016/j.catena.2011.05.022, 2011.

788 Bellin, N., Vanacker, V. and De Baets, S.: Anthropogenic and climatic impact on Holocene
789 sediment dynamics in SE Spain: A review, Quat. Int., 308–309, 112–129,
790 doi:10.1016/j.quaint.2013.03.015, 2013.

791 Beug, H.-J.: Leitfaden der Pollenbestimmung für Mitteleuropa und angrenzende Gebiete,
792 Fisch. Stuttg., 61, 2004.

793 Blaauw, M.: Methods and code for 'classical' age-modelling of radiocarbon sequences, Quat.
794 Geochronol., 5(5), 512–518, doi:https://doi.org/10.1016/j.quageo.2010.01.002, 2010.

795 Bond, G., Kromer, B., Beer, J., Muscheler, R., Evans, M. N., Showers, W., Hoffmann, S.,
796 Lotti-Bond, R., Hajdas, I. and Bonani, G.: Persistent Solar Influence on North Atlantic
797 Climate During the Holocene, Science, 294(5549), 2130, doi:10.1126/science.1065680,
798 2001.

799 Booth, R. K., Jackson, S. T., Forman, S. L., Kutzbach, J. E., E. A. Bettis, I., Kreigs, J. and
800 Wright, D. K.: A severe centennial-scale drought in midcontinental North America 4200
801 years ago and apparent global linkages, The Holocene, 15(3), 321–328,
802 doi:10.1191/0959683605hl825ft, 2005.

Bottema, S.: The interpretation of pollen spectra from prehistoric settlements (with special attention of Liguliflorae), Palaeohistoria, 17, 17–35, 1975.

Carrión, J. S.: Patterns and processes of Late Quaternary environmental change in a montane region of southwestern Europe, Quat. Sci. Rev., 21(18–19), 2047–2066, doi:https://doi.org/10.1016/S0277-3791(02)00010-0, 2002.

Carrión, J. S., Munuera, M., Dupré, M. and Andrade, A.: Abrupt vegetation changes in the Segura Mountains of southern Spain throughout the Holocene, J. Ecol., 89(5), 783–797, doi:10.1046/j.0022-0477.2001.00601.x, 2001b.

Carrión, J. S., Andrade, A., Bennett, K. D., Navarro, C. and Munuera, M.: Crossing forest thresholds: inertia and collapse in a Holocene sequence from south-central Spain, The Holocene, 11(6), 635–653, doi:10.1191/09596830195672, 2001a.

Carrión, J. S., Fernández, S., Jiménez-Moreno, G., Fauquette, S., Gil-Romera, G., González-Sampériz, P. and Finlayson, C.: The historical origins of aridity and vegetation degradation in southeastern Spain, J. Arid Environ., 74(7), 731–736, doi:https://doi.org/10.1016/j.jaridenv.2008.11.014, 2010a.

Carrión, J. S., Sánchez-Gómez, P., Mota, J. F., Yll, R. and Chaín, C.: Holocene vegetation dynamics, fire and grazing in the Sierra de Gádor, southern Spain, Holocene, 13(6), 839–849, doi:10.1191/0959683603hl662rp, 2003.

Carrión, J. S., Fuentes, N., González-Sampériz, P., Quirante, L. S., Finlayson, J. C., Fernández, S. and Andrade, A.: Holocene environmental change in a montane region of southern Europe with a long history of human settlement, Quat. Sci. Rev., 26(11–12), 1455–1475, doi:https://doi.org/10.1016/j.quascirev.2007.03.013, 2007.

Castillo Martín, A., Benavente Herrera, J., Fernández Rubio, R. and Pulido Bosch, A.: Evolución y ámbito hidrogeológico de la laguna de Padul (Granada), Las Zonas Húmedas En Andal. Monogr. DGMA-MOPU, 1984.

Combourieu-Nebout, N., Peyron, O., Dormoy, I., Desprat, S., Beaudouin, C., Kotthoff, U. and Marret, F.: Rapid climatic variability in the west Mediterranean during the last 25 000 years from high resolution pollen data, Clim Past, 5(3), 503–521, doi:10.5194/cp-5-503-2009, 2009.

Corella, J. P., Stefanova, V., El Anjoumi, A., Rico, E., Giralt, S., Moreno, A., Plata-Montero, A. and Valero-Garcés, B. L.: A 2500-year multi-proxy reconstruction of climate change and human activities in northern Spain: The Lake Arreo record, Palaeogeogr. Palaeoclimatol. Palaeoecol., 386, 555–568, doi:10.1016/j.palaeo.2013.06.022, 2013.

Currás, A., Zamora, L., Reed, J. M., García-Soto, E., Ferrero, S., Armengol, X., Mezquita-Joanes, F., Marqués, M. A., Riera, S. and Julià, R.: Climate change and human impact in central Spain during Roman times: High-resolution multi-proxy analysis of a tufa lake record (Somolinos, 1280m asl), Catena, 89(1), 31–53, doi:10.1016/j.catena.2011.09.009, 2012.

Damon, P. E. and Sonett, C. P.: Solar and terrestrial components of the atmospheric C-14 variation spectrum. In: Sonett, C.P., Giampapa, M.S., Matthews, M.S. (Eds.), The Sun in Time. University of Arizona Press, Tucson, AZ, USA., 1991.

843 Debret, M., Bout-Roumazeilles, V., Grousset, F., Desmet, M., McManus, J. F., Massei, N.,
844 Sebag, D., Petit, J.-R., Copard, Y. and Trentesaux, A.: The origin of the 1500-year climate
845 cycles in holocene north-atlantic records, Clim. Past, 3(4), 569–575, 2007.

846 Debret, M., Sebag, D., Crosta, X., Massei, N., Petit, J.-R., Chapron, E. and Bout-
847 Roumazeilles, V.: Evidence from wavelet analysis for a mid-Holocene transition in global
848 climate forcing, Quat. Sci. Rev., 28(25–26), 2675–2688,
849 doi:https://doi.org/10.1016/j.quascirev.2009.06.005, 2009.

850 Delgado, J., Alfaro, P., Galindo-Zaldivar, J., Jabaloy, A., Lopez Garrido, A. and Sanz de
851 Galdeano, C.: Structure of the Padul-Nigüelas basin (S Spain) from H/V ratios of ambient
852 noise: application of the method to study peat and coarse sediments, Pure Appl. Geophys.,
853 159(11), 2733–2749, 2002.

854 Domingo-García, M., Fernández-Rubio, R., Lopez, J. and González, C.: Aportación al
855 conocimiento de la Neotectónica de la Depresión del Padul (Granada), Tecniterrae, 53, 6–16,
856 1983.

857 Ejarque, A., Anderson, R. S., Simms, A. R. and Gentry, B. J.: Prehistoric fires and the
858 shaping of colonial transported landscapes in southern California: A paleoenvironmental
859 study at Dune Pond, Santa Barbara County, Quat. Sci. Rev., 112, 181–196,
860 doi:https://doi.org/10.1016/j.quascirev.2015.01.017, 2015.

861 El Aallali, A., Nieto, J. M. L., Raya, F. A. P. and Mesa, J. M.: Estudio de la vegetación
862 forestal en la vertiente sur de Sierra Nevada (Alpujarra Alta granadina), Itinera Geobot., (11),
863 387–402, 1998.

864 Faegri, K. and Iversen, J.: Textbook of Pollen Analysis. Wiley, New York., 1989.

865 Fletcher, W. J. and Sánchez-Goñi, M. F.: Orbital- and sub-orbital-scale climate impacts on
866 vegetation of the western Mediterranean basin over the last 48,000 yr, Quat. Res., 70(3),
867 451–464, doi:10.1016/j.yqres.2008.07.002, 2008.

868 Fletcher, W. J., Debret, M. and Sánchez-Goñi, M. F.: Mid-Holocene emergence of a low-
869 frequency millennial oscillation in western Mediterranean climate: Implications for past
870 dynamics of the North Atlantic atmospheric westerlies, The Holocene, 23(2), 153–166,
871 doi:10.1177/0959683612460783, 2013.

872 Florenzano, A., Marignani, M., Rosati, L., Fascetti, S. and Mercuri, A. M.: Are Cichorieae an
873 indicator of open habitats and pastoralism in current and past vegetation studies?, Plant
874 Biosyst. - Int. J. Deal. Asp. Plant Biol., 149(1), 154–165,
875 doi:10.1080/11263504.2014.998311, 2015.

876 Florschütz, F., Amor, J. M. and Wijmstra, T. A.: Palynology of a thick quaternary succession
877 in southern Spain, Palaeogeogr. Palaeoclimatol. Palaeoecol., 10(4), 233–264,
878 doi:http://dx.doi.org/10.1016/0031-0182(71)90049-6, 1971.

879 García-Alix, A., Jimenez-Espejo, F. J., Lozano, J. A., Jiménez-Moreno, G., Martinez-Ruiz,
880 F., Sanjuán, L. G., Jiménez, G. A., Alfonso, E. G., Ruiz-Puertas, G. and Anderson, R. S.:
881 Anthropogenic impact and lead pollution throughout the Holocene in Southern Iberia, Sci.
882 Total Environ., 449, 451–460, doi:https://doi.org/10.1016/j.scitotenv.2013.01.081, 2013.

883   García-Alix, A., Jiménez-Espejo, F. J., Toney, J. L., Jiménez-Moreno, G., Ramos-Román, M.
884   J., Anderson, R. S., Ruano, P., Queralt, I., Delgado Huertas, A. and Kuroda, J.: Alpine bogs
885   of southern Spain show human-induced environmental change superimposed on long-term
886   natural variations, Sci. Rep., 7(1), 7439, doi:10.1038/s41598-017-07854-w, 2017.

887   van Geel, B., Hallewas, D. P. and Pals, J. P.: A late holocene deposit under the Westfriese
888   Zeedijk near Enkhuizen (Prov. of Noord-Holland, The Netherlands): Palaeoecological and
889   archaeological aspects, Rev. Palaeobot. Palynol., 38(3), 269–335,
890   doi:http://dx.doi.org/10.1016/0034-6667(83)90026-X, 1983.

891   van Geel, B., Coope, G. R. and Hammen, T. V. D.: Palaeoecology and stratigraphy of the
892   lateglacial type section at Usselo (the Netherlands), Rev. Palaeobot. Palynol., 60(1), 25–129,
893   doi:http://dx.doi.org/10.1016/0034-6667(89)90072-9, 1989.

894   Gil García, M. J., Ruiz Zapata, M. B., Santisteban, J. I., Mediavilla, R., López-Pamo, E. and
895   Dabrio, C. J.: Late holocene environments in Las Tablas de Daimiel (south central Iberian
896   peninsula, Spain), Veg. Hist. Archaeobotany, 16(4), 241–250, doi:10.1007/s00334-006-0047-
897   9, 2007.

898   Gil-Romera, G., Carrión, J. S., Pausas, J. G., Sevilla-Callejo, M., Lamb, H. F., Fernández, S.
899   and Burjachs, F.: Holocene fire activity and vegetation response in South-Eastern Iberia,
900   Quat. Sci. Rev., 29(9), 1082–1092, doi:10.1016/j.quascirev.2010.01.006, 2010.

901   Grimm, E. C.: CONISS: a FORTRAN 77 program for stratigraphically constrained cluster
902   analysis by the method of incremental sum of squares, Comput. Geosci., 13(1), 13–35,
903   doi:http://dx.doi.org/10.1016/0098-3004(87)90022-7, 1987.

904   Guy-Ohlson, D.: Botryococcus as an aid in the interpretation of palaeoenvironment and
905   depositional processes, Rev. Palaeobot. Palynol., 71(1), 1–15,
906   doi:http://dx.doi.org/10.1016/0034-6667(92)90155-A, 1992.

907   Hurrell, J. W.: Decadal Trends in the North Atlantic Oscillation: Regional Temperatures and
908   Precipitation, Science, 269(5224), 676, doi:10.1126/science.269.5224.676, 1995.

909   Jalut, G., Dedoubat, J. J., Fontugne, M. and Otto, T.: Holocene circum-Mediterranean
910   vegetation changes: Climate forcing and human impact, Quat. Int., 200(1–2), 4–18,
911   doi:https://doi.org/10.1016/j.quaint.2008.03.012, 2009.

912   Jiménez-Espejo, F. J., García-Alix, A., Jiménez-Moreno, G., Rodrigo-Gámiz, M., Anderson,
913   R. S., Rodríguez-Tovar, F. J., Martínez-Ruiz, F., Giralt, S., Delgado Huertas, A. and Pardo-
914   Igúzquiza, E.: Saharan aeolian input and effective humidity variations over western Europe
915   during the Holocene from a high altitude record, Chem. Geol., 374–375, 1–12,
916   doi:10.1016/j.chemgeo.2014.03.001, 2014.

917   Jiménez-Moreno, G. and Anderson, R. S.: Holocene vegetation and climate change recorded
918   in alpine bog sediments from the Borreguiles de la Virgen, Sierra Nevada, southern Spain,
919   Quat. Res., 77(1), 44–53, doi:10.1016/j.yqres.2011.09.006, 2012.

920   Jiménez-Moreno, G., García-Alix, A., Hernández-Corbalán, M. D., Anderson, R. S. and
921   Delgado-Huertas, A.: Vegetation, fire, climate and human disturbance history in the
922   southwestern Mediterranean area during the late Holocene, Quat. Res., 79(2), 110–122,
923   doi:https://doi.org/10.1016/j.yqres.2012.11.008, 2013.

924 Jiménez-Moreno, G., Rodríguez-Ramírez, A., Pérez-Asensio, J. N., Carrión, J. S., López-
925 Sáez, J. A., Villarías-Robles, J. J. R., Celestino-Pérez, S., Cerrillo-Cuenca, E., León, Á. and
926 Contreras, C.: Impact of late-Holocene aridification trend, climate variability and
927 geodynamic control on the environment from a coastal area in SW Spain, Holocene, 25(4),
928 607–617, doi:10.1177/0959683614565955, 2015.

929 Kalugin, I., Daryin, A., Smolyaninova, L., Andreev, A., Diekmann, B. and Khlystov, O.:
930 800-yr-long records of annual air temperature and precipitation over southern Siberia inferred
931 from Teletskoye Lake sediments, Quat. Res., 67(3), 400–410,
932 doi:https://doi.org/10.1016/j.yqres.2007.01.007, 2007.

933 Laskar, J., Robutel, P., Joutel, F., Gastineau, M., Correia, A. C. M. and Levrard, B.: A long-
934 term numerical solution for the insolation quantities of the Earth, A&A, 428(1), 261–285,
935 doi:10.1051/0004-6361:20041335, 2004.

936 Lebreiro, S. M., Francés, G., Abrantes, F. F. G., Diz, P., Bartels-Jónsdóttir, H. B.,
937 Stroynowski, Z. N., Gil, I. M., Pena, L. D., Rodrigues, T., Jones, P. D., Nombela, M. A.,
938 Alejo, I., Briffa, K. R., Harris, I. and Grimalt, J. O.: Climate change and coastal hydrographic
939 response along the Atlantic Iberian margin (Tagus Prodelta and Muros Ría) during the last
940 two millennia, Holocene, 16(7), 1003–1015, doi:10.1177/0959683606hl990rp, 2006.

941 Lillios, K. T., Blanco-González, A., Drake, B. L. and López-Sáez, J. A.: Mid-late Holocene
942 climate, demography, and cultural dynamics in Iberia: A multi-proxy approach, Quat. Sci.
943 Rev., 135, 138–153, doi:https://doi.org/10.1016/j.quascirev.2016.01.011, 2016.

944 López-Sáez, J. A., Abel-Schaad, D., Pérez-Díaz, S., Blanco-González, A., Alba-Sánchez, F.,
945 Dorado, M., Ruiz-Zapata, B., Gil-García, M. J., Gómez-González, C. and Franco-Múgica, F.:
946 Vegetation history, climate and human impact in the Spanish Central System over the last
947 9000 years, Quat. Int., 353, 98–122, doi:https://doi.org/10.1016/j.quaint.2013.06.034, 2014.

948 Lukianova, R. and Alekseev, G.: Long-Term Correlation Between the Nao and Solar
949 Activity, Sol. Phys., 224(1), 445–454, doi:10.1007/s11207-005-4974-x, 2004.

950 Magny, M.: Holocene climate variability as reflected by mid-European lake-level
951 fluctuations and its probable impact on prehistoric human settlements, Quat. Int., 113(1), 65–
952 79, doi:https://doi.org/10.1016/S1040-6182(03)00080-6, 2004.

953 Magny, M., Peyron, O., Sadori, L., Ortu, E., Zanchetta, G., Vannière, B. and Tinner, W.:
954 Contrasting patterns of precipitation seasonality during the Holocene in the south- and north-
955 central Mediterranean, J. Quat. Sci., 27(3), 290–296, doi:10.1002/jqs.1543, 2012.

956 Magri, D.: Late Quaternary vegetation history at Lagaccione near Lago di Bolsena (central
957 Italy), Rev. Palaeobot. Palynol., 106(3–4), 171–208, doi:https://doi.org/10.1016/S0034-
958 6667(99)00006-8, 1999.

959 Marchal, O., Cacho, I., Stocker, T. F., Grimalt, J. O., Calvo, E., Martrat, B., Shackleton, N.,
960 Vautravers, M., Cortijo, E., Van Kreveld, S., Andersson, C., Koç, N., Chapman, M., Sbaffi,
961 L., Duplessy, J.-C., Sarnthein, M., Turon, J.-L., Duprat, J. and Jansen, E.: Apparent long-term
962 cooling of the sea surface in the northeast Atlantic and Mediterranean during the Holocene,
963 Quat. Sci. Rev., 21(4–6), 455–483, doi:10.1016/S0277-3791(01)00105-6, 2002.

964 Martín-Puertas, C., Valero-Garcés, B. L., Mata, M. P., González-Sampériz, P., Bao, R.,
965 Moreno, A. and Stefanova, V.: Arid and humid phases in southern Spain during the last 4000
966 years: the Zoñar Lake record, Córdoba, The Holocene, 18(6), 907–921,
967 doi:10.1177/0959683608093533, 2008.

968 Martín-Puertas, C., Valero-Garcés, B. L., Brauer, A., Mata, M. P., Delgado-Huertas, A. and
969 Dulski, P.: The Iberian-Roman Humid Period (2600-1600 cal yr BP) in the Zoñar Lake varve
970 record (Andalucía, southern Spain), Quat. Res., 71(2), 108–120,
971 doi:10.1016/j.yqres.2008.10.004, 2009.

972 Martín-Puertas, C., Valero-Garcés, B. L., Mata, M. P., Moreno, A., Giralt, S., Martínez-Ruiz,
973 F. and Jiménez-Espejo, F.: Geochemical processes in a Mediterranean Lake: A high-
974 resolution study of the last 4,000 years in Zoñar Lake, southern Spain, J. Paleolimnol., 46(3),
975 405–421, doi:10.1007/s10933-009-9373-0, 2011.

976 Mayewski, P. A., Rohling, E. E., Stager, J. C., Karlén, W., Maasch, K. A., Meeker, L. D.,
977 Meyerson, E. A., Gasse, F., Kreveld, S. van, Holmgren, K., Lee-Thorp, J., Rosqvist, G.,
978 Rack, F., Staubwasser, M., Schneider, R. R. and Steig, E. J.: Holocene climate variability,
979 Quat. Res., 62(3), 243–255, doi:https://doi.org/10.1016/j.yqres.2004.07.001, 2004.

980 Mercuri, A. M., Accorsi, C. A., Mazzanti, M. B., Bosi, G., Cardarelli, A., Labate, D.,
981 Marchesini, M. and Grandi, G. T.: Economy and environment of Bronze Age settlements –
982 Terramaras – on the Po Plain (Northern Italy): first results from the archaeobotanical research
983 at the Terramara di Montale, Veg. Hist. Archaeobotany, 16(1), 43, doi:10.1007/s00334-006-
984 0034-1, 2006.

985 Morellón, M., Valero-Garcés, B., Vegas-Vilarrúbia, T., González-Sampériz, P., Romero, Ó.,
986 Delgado-Huertas, A., Mata, P., Moreno, A., Rico, M. and Corella, J. P.: Lateglacial and
987 Holocene palaeohydrology in the western Mediterranean region: The Lake Estanya record
988 (NE Spain), Quat. Sci. Rev., 28(25–26), 2582–2599,
989 doi:https://doi.org/10.1016/j.quascirev.2009.05.014, 2009.

990 Morellón, M., Valero-Garcés, B., González-Sampériz, P., Vegas-Vilarrúbia, T., Rubio, E.,
991 Rieradevall, M., Delgado-Huertas, A., Mata, P., Romero, Ó., Engstrom, D. R., López-
992 Vicente, M., Navas, A. and Soto, J.: Climate changes and human activities recorded in the
993 sediments of Lake Estanya (NE Spain) during the Medieval Warm Period and Little Ice Age,
994 J. Paleolimnol., 46(3), 423–452, doi:10.1007/s10933-009-9346-3, 2011.

995 Morellón, M., Anselmetti, F. S., Ariztegui, D., Brushulli, B., Sinopoli, G., Wagner, B.,
996 Sadori, L., Gilli, A. and Pambuku, A.: Human–climate interactions in the central
997 Mediterranean region during the last millennia: The laminated record of Lake Butrint
998 (Albania), Spec. Issue Mediterr. Holocene Clim. Environ. Hum. Soc., 136(Supplement C),
999 134–152, doi:10.1016/j.quascirev.2015.10.043, 2016.

1000 Moreno, A., Cacho, I., Canals, M., Grimalt, J. O., Sánchez-Goñi, M. F., Shackleton, N. and
1001 Sierro, F. J.: Links between marine and atmospheric processes oscillating on a millennial
1002 time-scale. A multi-proxy study of the last 50,000 yr from the Alboran Sea (Western
1003 Mediterranean Sea), Quat. Sci. Rev., 24(14–15), 1623–1636,
1004 doi:https://doi.org/10.1016/j.quascirev.2004.06.018, 2005.

Moreno, A., Pérez, A., Frigola, J., Nieto-Moreno, V., Rodrigo-Gámiz, M., Martrat, B., González-Sampériz, P., Morellón, M., Martín-Puertas, C., Corella, J. P., Belmonte, Á., Sancho, C., Cacho, I., Herrera, G., Canals, M., Grimalt, J. O., Jiménez-Espejo, F., Martínez-Ruiz, F., Vegas-Vilarrúbia, T. and Valero-Garcés, B. L.: The Medieval Climate Anomaly in the Iberian Peninsula reconstructed from marine and lake records, Quat. Sci. Rev., 43, 16–32, doi:https://doi.org/10.1016/j.quascirev.2012.04.007, 2012.

Nestares, T. and Torres, T. de: Un nuevo sondeo de investigación paleoambiental del Pleistoceno y Holoceno en la turbera del Padul (Granada, Andalucía). Geogaceta 23, 99-102., 1997.

Oliva, M., Schulte, L. and Ortiz, A. G.: Morphometry and Late Holocene activity of solifluction landforms in the Sierra Nevada, Southern Spain, Permafr. Periglac. Process., 20(4), 369–382, 2009.

Olsen, J., Anderson, N. J. and Knudsen, M. F.: Variability of the North Atlantic Oscillation over the past 5,200 years, Nat. Geosci, 5(11), 808–812, doi:10.1038/ngeo1589, 2012.

Ortiz, J. E., Torres, T., Delgado, A., Julià, R., Lucini, M., Llamas, F. J., Reyes, E., Soler, V. and Valle, M.: The palaeoenvironmental and palaeohydrological evolution of Padul Peat Bog (Granada, Spain) over one million years, from elemental, isotopic and molecular organic geochemical proxies, Org. Geochem., 35(11–12), 1243–1260, doi:https://doi.org/10.1016/j.orggeochem.2004.05.013, 2004.

Paillard, D., Labeyrie, L. and Yiou, P.: Macintosh Program performs time-series analysis, Eos Trans. Am. Geophys. Union, 77(39), 379–379, doi:10.1029/96EO00259, 1996.

Pérez Raya, F. and López Nieto, J.: Vegetación acuática y helofítica de la depresión de Padul (Granada), Acta Bot Malacit., 16(2), 373–389, 1991.

Pons, A. and Reille, M.: The holocene- and upper pleistocene pollen record from Padul (Granada, Spain): A new study, Palaeogeogr. Palaeoclimatol. Palaeoecol., 66(3), 243–263, doi:http://dx.doi.org/10.1016/0031-0182(88)90202-7, 1988.

Ramos-Román, M. J., Jiménez-Moreno, G., Anderson, R. S., García-Alix, A., Toney, J. L., Jiménez-Espejo, F. J. and Carrión, J. S.: Centennial-scale vegetation and North Atlantic Oscillation changes during the Late Holocene in the southern Iberia, Quat. Sci. Rev., 143, 84–95, doi:https://doi.org/10.1016/j.quascirev.2016.05.007, 2016.

Reimer, P. J., Bard, E., Bayliss, A., Beck, J. W., Blackwell, P. G., Ramsey, C. B., Buck, C. E., Cheng, H., Edwards, R. L., Friedrich, M., Grootes, P. M., Guilderson, T. P., Haflidason, H., Hajdas, I., Hatté, C., Heaton, T. J., Hoffmann, D. L., Hogg, A. G., Hughen, K. A., Kaiser, K. F., Kromer, B., Manning, S. W., Niu, M., Reimer, R. W., Richards, D. A., Scott, E. M., Southon, J. R., Staff, R. A., Turney, C. S. M. and van der Plicht, J.: IntCal13 and Marine13 Radiocarbon Age Calibration Curves 0–50,000 Years cal BP, Radiocarbon, 55(4), 1869–1887, doi:10.2458/azu_js_rc.55.16947, 2013.

Riera, S., Wansard, G. and Julià, R.: 2000-year environmental history of a karstic lake in the Mediterranean Pre-Pyrenees: the Estanya lakes (Spain), {CATENA}, 55(3), 293–324, doi:https://doi.org/10.1016/S0341-8162(03)00107-3, 2004.

Riera, S., López-Sáez, J. A. and Julià, R.: Lake responses to historical land use changes in northern Spain: The contribution of non-pollen palynomorphs in a multiproxy study, Rev. Palaeobot. Palynol., 141(1–2), 127–137, doi:https://doi.org/10.1016/j.revpalbo.2006.03.014, 2006.

Roberts, N., Brayshaw, D., Kuzucuoğlu, C., Perez, R. and Sadori, L.: The mid-Holocene climatic transition in the Mediterranean: Causes and consequences, The Holocene, 21(1), 3–13, doi:10.1177/0959683610388058, 2011.

Rodrigo-Gámiz, M., Martínez-Ruiz, F., Rodríguez-Tovar, F. J., Jiménez-Espejo, F. J. and Pardo-Igúzquiza, E.: Millennial- to centennial-scale climate periodicities and forcing mechanisms in the westernmost Mediterranean for the past 20,000 yr, Quat. Res., 81(1), 78–93, doi:https://doi.org/10.1016/j.yqres.2013.10.009, 2014.

Sadori, L., Jahns, S. and Peyron, O.: Mid-Holocene vegetation history of the central Mediterranean, The Holocene, 21(1), 117–129, doi:10.1177/0959683610377530, 2011.

Sadori, L., Giraudi, C., Masi, A., Magny, M., Ortu, E., Zanchetta, G. and Izdebski, A.: Climate, environment and society in southern Italy during the last 2000 years. A review of the environmental, historical and archaeological evidence, Spec. Issue Mediterr. Holocene Clim. Environ. Hum. Soc., 136(Supplement C), 173–188, doi:10.1016/j.quascirev.2015.09.020, 2016.

Sanz de Galdeano, C., El Hamdouni, R. and Chacón, J.: Neotectónica de la fosa del Padul y del Valle de Lecrín, Itiner. Geomorfológicos Por Andal. Orient. Publicacions Univ. Barc. Barc., 65–81, 1998.

Sicre, M.-A., Jalali, B., Martrat, B., Schmidt, S., Bassetti, M.-A. and Kallel, N.: Sea surface temperature variability in the North Western Mediterranean Sea (Gulf of Lion) during the Common Era, Earth Planet. Sci. Lett., 456, 124–133, doi:http://dx.doi.org/10.1016/j.epsl.2016.09.032, 2016.

Sonett, C. P. and Suess, H. E.: Correlation of bristlecone pine ring widths with atmospheric 14C variations: a climate-Sun relation, Nature, 307(5947), 141–143, doi:10.1038/307141a0, 1984.

Steinhilber, F., Beer, J. and Fröhlich, C.: Total solar irradiance during the Holocene, Geophys. Res. Lett., 36(19), n/a–n/a, doi:10.1029/2009GL040142, 2009.

Trouet, V., Esper, J., Graham, N. E., Baker, A., Scourse, J. D. and Frank, D. C.: Persistent Positive North Atlantic Oscillation Mode Dominated the Medieval Climate Anomaly, Science, 324(5923), 78, doi:10.1126/science.1166349, 2009.

Valle, F.: Mapa de series de vegetación de Andalucía 1: 400 000, Editorial Rueda., 2003.

Valle Tendero, F.: Modelos de Restauración Forestal: Datos botánicos aplicados a la gestión del Medio Natural Andaluz II: Series de vegetación, Cons. Medio Ambiente Junta Andal. Sevilla, 2004.

Villegas Molina, F.: Laguna de Padul: Evolución geológico-histórica, Estud. Geográficos, 28(109), 561, 1967.

1084   Zanchettin, D., Rubino, A., Traverso, P. and Tomasino, M.: Impact of variations in solar
1085   activity on hydrological decadal patterns in northern Italy, J. Geophys. Res. Atmospheres,
1086   113(D12), n/a–n/a, doi:10.1029/2007JD009157, 2008.

Figures and tables
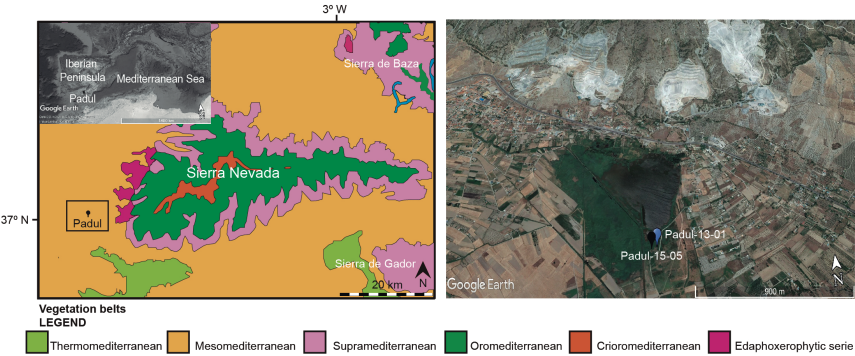
Figure 1. Location of Padul in Sierra Nevada, southern Iberian Peninsula. Panel on the left is the map of the vegetation belts in the Sierra Nevada (Modified from REDIAM. Map of the vegetation series of Andalucía: http://laboratoriorediam.cica.es/VisorGenerico/?tipo=WMS&url=http://www.juntadeandaluci a.es/medioambiente/mapwms/REDIAM_Series_Vegetacion_Andalucia?). The inset map is the Google earth image of the Iberian Peninsula in the Mediterranean region. Panel on the right is the Google earth image (http://www.google.com/earth/index.html) of Padul peat bog area showing the coring locations.
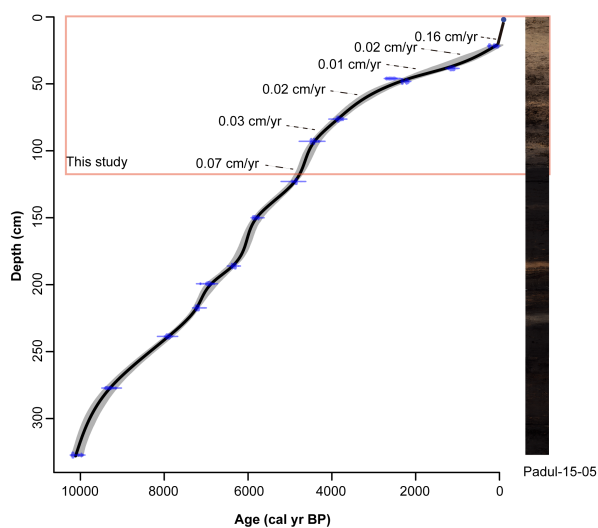
1097

1098 **Figure 2.** Photo of the Padul-15-05 sediment core with the age-depth model showing the part
1099 of the record that was studied here (red rectangle). The sediment accumulation rates (SAR)
1100 between individual segments are marked. See the body of the text for the explanation of the
1101 age reconstructions.

1102

1103

1104

1105 **Figure 3.** Lithology, facies interpretation with paleontology, magnetic susceptibility (MS),
1106 and geochemical (X-ray fluorescence (XRF) and total organic carbon (TOC) data from the
1107 Padul-15-05 record. XRF elements are represented normalized by the total counts. (a)
1108 Magnetic susceptibility (MS; SI units). (b) Strontium normalized (Sr; norm.). (c) Bromine
1109 norm. (Br; norm.). (d) Calcium normalized. (Ca; norm.). (e) Silica normalized (Si; norm.). (f)
1110 Potassium normalized (K; norm.). (g) Titanium normalized (Ti; norm.). (h) Iron normalized
1111 (Fe; norm.). (i) Zirconium normalized (Zr; norm.). (j) Total organic carbon (TOC %). AMS
1112 radiocarbon dates (cal yr BP) are shown on the left.

1113

1114

1115
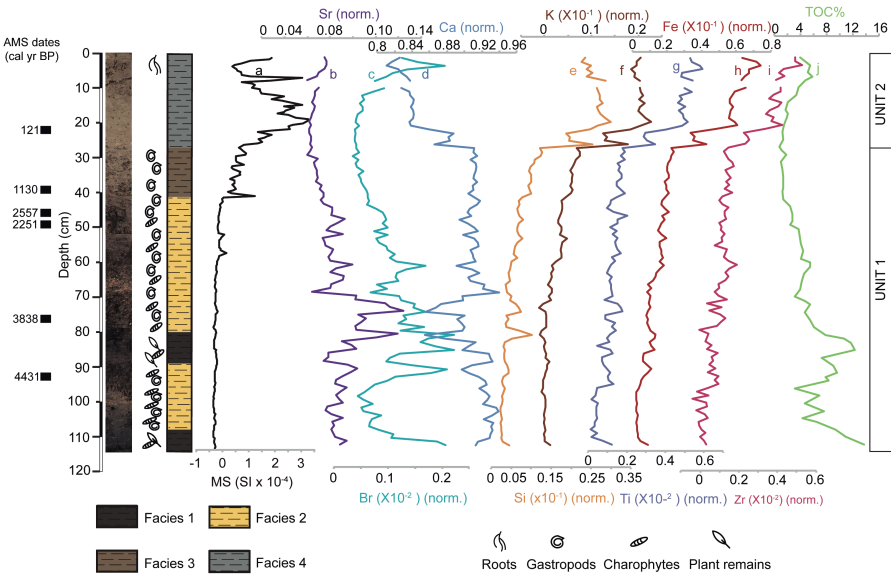
1116 **Figure 4.** Percentages of selected pollen taxa and non-pollen palynomorphs (NPPs) from the
1117 Padul-15-05 record, calculated with respect to terrestrial pollen sum. Silhouettes show 7-time
1118 exaggerations of pollen percentages. Pollen zonation, pollen concentration (grains/cc),
1119 lithology and AMS radiocarbon dates are shown on the right. Tree and shrubs are showing in
1120 green, herbs and grasses in yellow, aquatics in dark blue, algae in blue, fungi in brown and
1121 thecamoebians in beige. The Mediterranean forest taxa category is composed of *Quercus*
1122 total, *Olea*, *Phillyrea* and *Pistacia*. The xerophyte group includes *Artemisia, Ephedra*, and
1123 Amaranthaceae. PA = Pollen zones.

1124
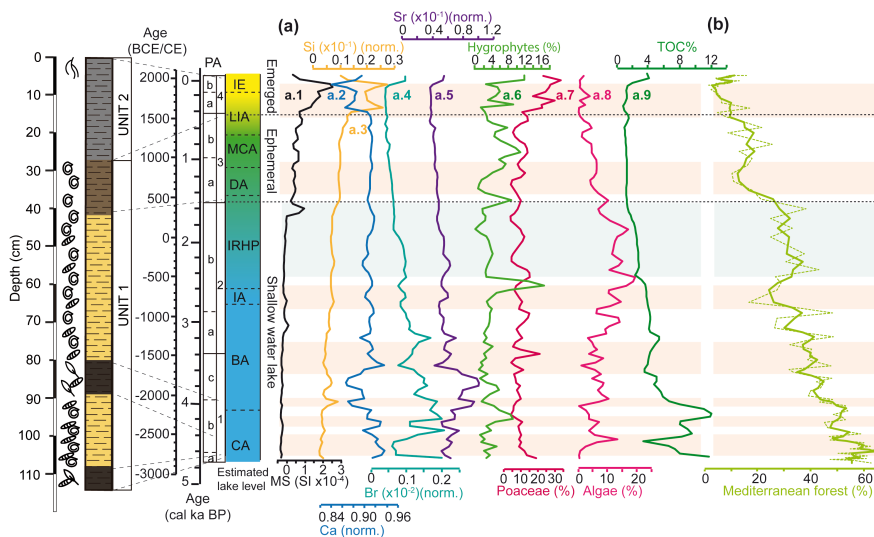
1125

Figure 5. Estimated lake level evolution and regional palynological component from the last ca. 4700 yr based on the synthesis of determinate proxies from the Padul-15-05 record: (a) Proxies used to estimate the water table evolution from the Padul-15-05 record (proxies were resampled at 50 yr (lineal interpolation) using Past software http://palaeo-electronica.org/2001_1/past/issue1_01.htm). [(a.1) Magnetic Susceptibility (MS) in SI; (a.2) Silica normalized (Si; norm.); (a.3) Calcium normalized (Ca; norm.); (a.4) Bromine normalized (Br; norm.); (a.5) Strontium normalized (Sr; norm.); (a.6) Hygrophytes (%); (a.7) Poaceae (%); (a.8) Algae (%) (a.9) Total organic carbon (TOC %)] (b) Mediterranean forest taxa, with a smoothing of three-point in bold. Pink and blue shading indicates Holocene arid and humid regionally events, respectively. See the body of the text for the explanation of the lake level reconstruction. Mediterranean forest smoothing was made using Analyseries software (Paillard et al., 1996). PA = Pollen Zones; CA = Copper Age; BA = Bronze Age; IA = Iron Age; IRHP = Iberian Roman Humid Period; DA = Dark Ages; MCA = Medieval Climate Anomaly; LIA = Little Ice Age; IE = Industrial Era.
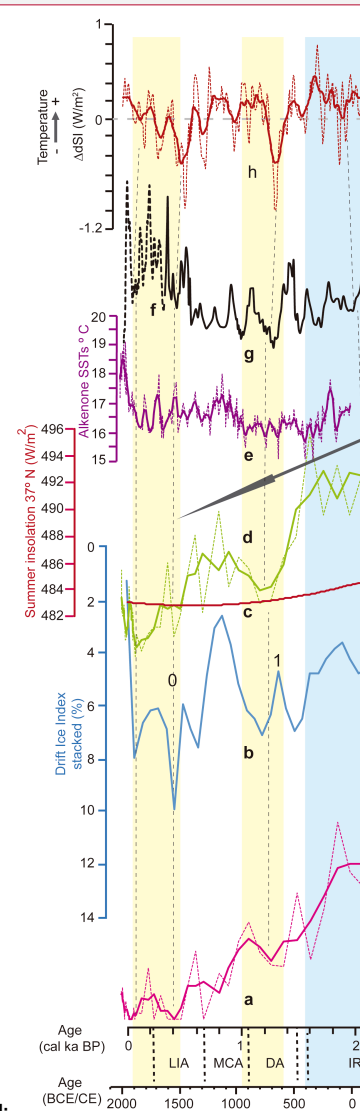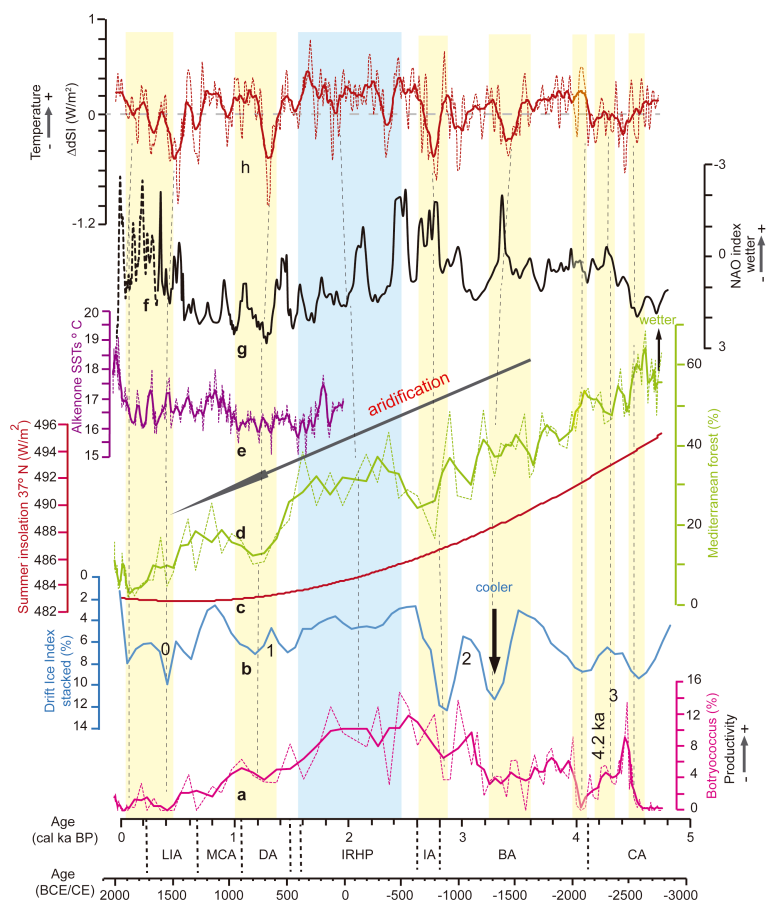
Figure 6. Comparison of the last ca. 4700 yr between different pollen taxa from the Padul-15-05 record, summer insolation for the Sierra Nevada latitude, eastern Mediterranean humidity and North Atlantic temperature. (a) *Botryococcus* from the Padul-15-05 record, with a smoothing of three-point in bold (this study). (b) Drift Ice Index (reversed) from the North Atlantic (Bond et al., 2001). (c) Summer insolation calculated for 37º N (Laskar et al., 2004). (d) Mediterranean forest taxa from the Padul-15-05 record, with a smoothing of three-point in bold (this study). (e) Alkenone-SSTs from the Gulf of Lion (Sicre et al., 2016), with a smoothing of four-point in bold. (f) North Atlantic Oscillation (NAO) index from a climate proxy reconstruction from Morocco and Scotland (Trouet et al., 2009). (g) North Atlantic Oscillation (NAO) index (reversed) from a climate proxy reconstruction from Greenland (Olsen et al., 2012). (h) Total solar irradiance reconstruction from cosmogenic radionuclide from a Greenland ice core (Steinhilber et al., 2009), with a smoothing of twenty-one-point in bold. Note that the magnitude of the different curves is not in the same scale. Yellow and

blue shading correspond with arid (and cold) and humid (and warm) periods, respectively. Grey dash lines show a tentative correlation between arid and cold conditions and the decrease in the Mediterranean forest and *Botryococcus*. Mediterranean forest, *Botryococcus* and solar irradiance smoothing was made using Analyseries software (Paillard et al., 1996), Alkenone-SSTs smoothing was made using Past software (http://palaeo-electronica.org/2001_1/past/issue1_01.htm). A linear r (Pearson) correlation was calculated between *Botryococcus* (detrended) and Drift Ice Index (Bond et al., 2001; r = -0.63; $p <$ 0.0001; between ca. 4700 to 1500 cal ka BP – r=-0.48; $p < 0.0001$ between 4700 and -65 cal yr BP). Previously, the data were detrended (only in *Botryococcus*), resampled at 70-yr (linear interpolation) in order to obtain equally spaced time series and smoothed to three-point average. CA = Copper Age; BA = Bronze Age; IA = Iron Age; IRHP = Iberian Roman Humid Period; DA = Dark Ages; MCA = Medieval Climate Anomaly; LIA = Little Ice Age; IE = Industrial Era.

1171
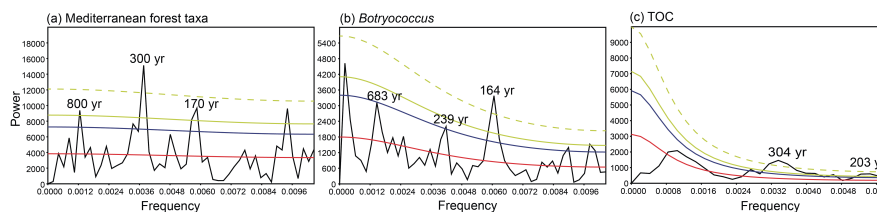
Figure 7. Spectral analysis of (a) Mediterranean forest taxa and (b) *Botryococcus* (mean sampling space = 47 yr) and (c) TOC (mean sampling space = 78 yr) from the Padul-15-05. The significant periodicities above confident level are shown. Confidence level 90 % (blue line), 95 % (green line), 99 % (green dash line) and AR (1) red noise (red line). Spectral analysis was made with Past software (http://palaeo-electronica.org/2001_1/past/issue1_01.htm).

1178
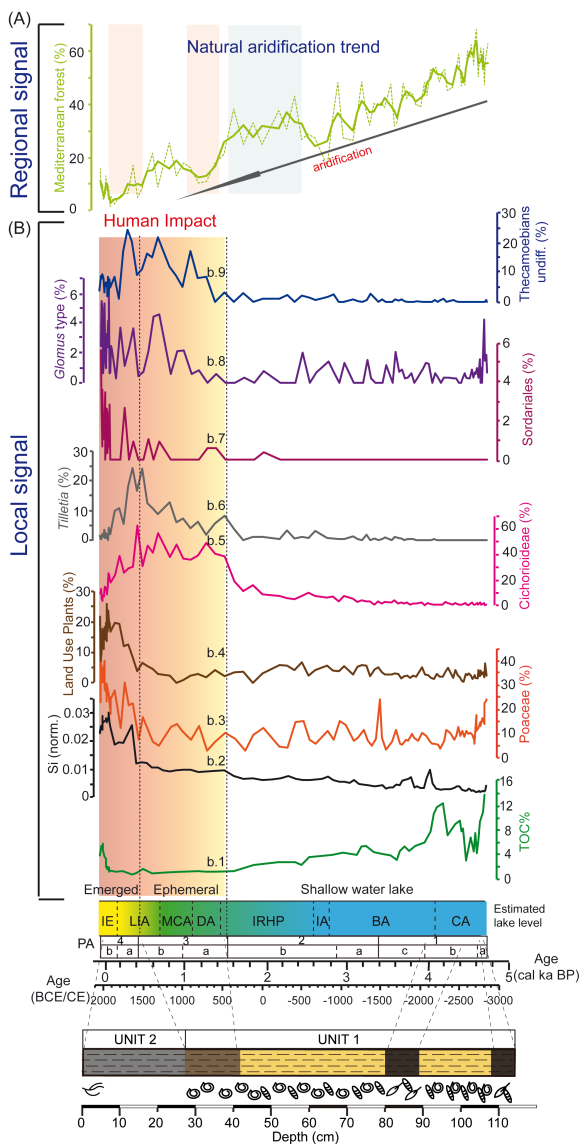
1179

Figure 8. Comparison of the last ca. 4700 yr between regional climatic proxies and local human activity indicators from the Padul-15-05 record. (A) Mediterranean forest taxa, with a smoothing of three-point in bold. (B) Local human activities indicators [(b.1) Total organic carbon (TOC %), soil erosion indicator; (b.2) Si normalized (Si, norm.), soil erosion indicator; (b.3) Poaceae (%), lake drained and/or cultivars indicator; (b.4) Land Use Plants (%), cultivar indicator; (b.5) Cichorioideae (%), livestock occurrence indicator; (b.6) *Tilletia*

1186 (%), farming indicator; (b.7) Sordariales (%), livestock indicator; (b.8) *Glomus* type, soil
1187 erosion, (b.9) Thecamoebians undiff. (%), livestock indicator]. Degraded yellow to red
1188 shading correspond with the time when we have evidence of human shaping the environment
1189 since ca. 1550 cal yr BP to Present. Previously to that period there is a lack of clear evidences
1190 of human impact in the area. Land use plants is composed by Polygonaceae, Amaranthaceae,
1191 Convolvulaceae, *Plantago*, Apiaceae and Cannabaceae-Urticaceae type.

1192 **Table 1.** Age data for Padul-15-05 record. All ages were calibrated using R-code package
1193 'clam 2.2' employing the calibration curve IntelCal 13 (Reimer et al., 2013) at 95 % of
1194 confident range.

1195 *Sample number assigned at radiocarbon laboratory

Laboratory number	Core	Material	Depth (cm)	Age (^{14}C yr BP ± 1σ)	Calibrated age (cal yr BP) 95 % confidence interval	Median age (cal yr BP)
Reference ages			0	2015CE	-65	-65
D-AMS 008531	Padul-13-01	Plant remains	21.67	103 ± 24	23-264	127
Poz-77568	Padul-15-05	Org. bulk sed.	38.46	1205 ± 30	1014-1239	1130
BETA-437233	Padul-15-05	Plant remains	46.04	2480 ± 30	2385-2722	2577
Poz-77569	Padul-15-05	Org. bulk sed.	48.21	2255 ± 30	2158-2344	2251
BETA-415830	Padul-15-05	Shell	71.36	3910 ± 30	4248-4421	4343
BETA- 437234	Padul-15-05	Plant remains	76.34	3550 ± 30	3722-3956	3838
BETA-415831	Padul-15-05	Org. bulk sed.	92.94	3960 ± 30	4297-4519	4431
Poz-74344	Padul-15-05	Plant remains	122.96	4295 ± 35	4827-4959	4871
BETA-415832	Padul-15-05	Plant remains	150.04	5050 ± 30	5728-5900	5814
Poz-77571	Padul-15-05	Plant remains	186.08	5530 ± 40	6281-6402	6341
Poz-74345	Padul-15-05	Plant remains	199.33	6080 ± 40	6797-7154	6935
BETA-415833	Padul-15-05	Org. bulk sed.	217.36	6270 ± 30	7162-7262	7212
Poz-77572	Padul-15-05	Org. bulk sed.	238.68	7080 ± 50	7797-7999	7910
Poz-74347	Padul-15-05	Plant remains	277.24	8290 ± 40	9138-9426	9293
BETA-415834	Padul-15-05	Plant remains	327.29	8960 ± 30	9932-10221	10107

1196

1197

1198 **Table 2.** Linear r (Pearson) correlation between geochemical elements from the Padul-15-05
1199 record. Statistical treatment was performed using the Past software (http://palaeo-
1200 electronica.org/2001_1/past/issue1_01.htm).

1201

	Si	K	Ca	Ti	Fe	Zr	Br	Sr
Si		8.30E-80	2.87E-34	7.47E-60	3.22E-60	5.29E-44	0.001152	7.79E-09
K	0.98612		7.07E-29	6.05E-60	8.20E-68	1.77E-51	0.00030317	5.38E-12
Ca	-0.88096	-0.84453		6.09E-42	5.81E-39	8.10E-34	0.35819	0.26613
Ti	0.96486	0.96501	-0.91794		1.74E-74	1.12E-57	0.074223	8.88E-07
Fe	0.96546	0.97577	-0.90527	0.98224		2.77E-66	0.051072	3.32E-08
Zr	0.92566	0.94789	-0.8783	0.96109	0.97398		0.054274	7.16E-08
Br	-0.31739	-0.3506	-0.091917	-0.17755	-0.19372	-0.19116		4.03E-18
Sr	-0.53347	-0.61629	0.11113	-0.46426	-0.51386	-0.50295	0.72852	

1202

1203

1204

1205

1206

1207

1208

1209

1210

1211

1212

1213

1214

1215

1216

1217